Energy Reports 8 (2022) 10688–10704

Contents lists available at ScienceDirect

Energy Reports

journal homepage: www.elsevier.com/locate/egyr

Research paper

Kinetic synergistic effect in co-pyrolysis of *Eucalyptus globulus* with high and low density polyethylene

M. Ruiz-Montoya, A. Palma *, S. Lozano-Calvo, E. Morales, M.J. Díaz

Pro²TecS – Product Technology and Chemical Processes Research Centre, Department of Chemical Engineering, Physical Chemistry and Materials Science, University of Huelva, Campus "El Carmen", 21071, Huelva, Spain

ARTICLE INFO

Article history:
Received 5 November 2021
Received in revised form 14 July 2022
Accepted 13 August 2022
Available online xxxx

Keywords:
Eucalyptus globulus
Pyrolysis
HDPE
LDPE
Kinetic

ABSTRACT

The pyrolysis of *Eucalyptus globulus* (EG) with different blends of high density polyethylene (HDPE) and low density polyethylene (LDPE) by thermogravimetry has been studied. ASTM-E1641-16 standard method has been used to evaluate the kinetics during the pyrolysis of the studied blends. For all feedstocks (EG, HDPE and LDPE) and blends studied, the relative content (%) of the volatile organic compound has been determined by GC–MS analysis. Different synergistic effects on the activation energy of EG blends with HDPE and LDPE have been found. EG-HDPE blends showed a minimum activation energy (Ea) (125 kJ mol^{-1}) at the 80% EG–20% HDPE ratio, while the minimum Ea value for EG-LDPE blends was found at the 60% EG–40% LDPE ratio (135 kJ mol^{-1}) has been identified. To test which components exert a greater synergistic effect, mixtures of HDPE and LDPE with the main components of eucalyptus (cellulose, hemicellulose and lignin) have also been studied. However, no synergistic effects on the pyrolysis of cellulose have been detected. Moreover, in hemicellulose and lignin with both types of polyethylene mixtures, a significant decrease in Ea has been appreciated. The lowest Ea values for 60% cellulose–40% HDPE (167 kJ mol^{-1}) and 60% lignin–40% HDPE (140 kJ mol^{-1}) has been calculated. On the other hand, minimum values for 40% cellulose–60% LDPE (166 kJ mol^{-1}) mixture and for 40% lignin–60% LDPE (168 kJ mol^{-1}) mixture have been detected. Thus, the decrease in both Ea and the Arrhenius pre-exponential factor on the eucalyptus-polyethylene blends to the presence of hemicellulose and lignin can be attributed. Moreover, during the co-pyrolysis of HDPE-EG mixtures, n-paraffins, ketones, phenols and sugars are the main VOCs identified. In contrast, in LDPE-EG mixtures, only n-paraffins (55%) and olefins (44%) have been identified.

© 2022 The Author(s). Published by Elsevier Ltd. This is an open access article under the CC BY-NC-ND license (http://creativecommons.org/licenses/by-nc-nd/4.0/).

1. Introduction

Social, economic and environmental needs require a progressive reduction of energy dependence on fossil fuels. Such needs have promoted the development of research focused on new compounds production processes based on both biomass and/or organic waste as raw material (Popp et al., 2021). Moreover, fuels and chemicals derived from different types of biomass can play an important role in reducing CO_2 emissions and become a strategic source to provide energy competitiveness and environmental viability. However, in this area, it is still necessary to establish biomass utilization policies that consider its sustainable use, avoiding soil degradation and preventing competition with human and animal feed stuffs (Clauser et al., 2021; Dar et al., 2021).

Alternatively, although plastic waste management is improving, especially in developed countries, a relatively large portion of plastic waste is still sent to landfills in many countries. The management of plastic waste is largely determined by the nature of the initial material and its degradation degree, so the recycling or recovery of some types of plastics is proving to be both an industrial and environmental problem (Balaji and Liu, 2021). More specifically, in the EU, a large proportion of plastic waste is sent to landfills (Bishop et al., 2020).

Plastic recycling depends on the plastic chemical composition, but the possibilities of the recycling plastic waste are being unexploited in a large percentage (Balaji and Liu, 2021). This under-recycling or under-recovery is especially important for agro-industrial plastics, due, both to the large proportion of contaminants it contains and to their deterioration due to environmental conditions (Pazienza and De Lucia, 2020). In this respect, plastic materials made from both high and low density polyethylene (HDPE and LDPE respectively) are currently widely used in both films and materials commonly used in agriculture, becoming irreplaceable raw materials for agricultural production (Chow et al., 2018) becoming, due to their non-degradability,

* Corresponding author.
E-mail address: alberto.palma@diq.uhu.es (A. Palma).

https://doi.org/10.1016/j.egyr.2022.08.200
2352-4847/© 2022 The Author(s). Published by Elsevier Ltd. This is an open access article under the CC BY-NC-ND license (http://creativecommons.org/licenses/by-nc-nd/4.0/).

their elimination is a serious problem both environmentally and socially as well as wasteful of resources (Fa et al., 2019).

On the other hand, lignocellulosic biomass can be valued by different biological or thermochemical processes (Bueno et al., 2008; Delgado-Rodríguez et al., 2010). *Eucalyptus Globulus* is one of the most widespread species in the world, occupying more than 21 million hectares (FAO, 2022) because it is recognized as one of the fastest growing trees (Barrio-Anta et al., 2021). Moreover, a significant percentage of biomass has been found in this species ranging between 78%–82% for wood and 11%–20% for leaves and fine branches (Pérez-Cruzado et al., 2011).

Different processes for obtaining diverse products from biomass are often labeled biorefinery processes. In these processes, apart from direct energy, different chemical products, synthetic natural gas, bio-oils, light olefins, H_2, coke, etc., can be produced (Ferreira, 2017). Also, the production of energy and chemicals by thermochemical processes has been extensively studied (Rodríguez-Luna et al., 2021; Zhang et al., 2020) and this pathway is a promising route for plastic valorization. In this sense, among the thermochemical processes with major biomass valorization potential are pyrolytic processes (Antelava et al., 2021). Pyrolysis is a process in which organic matter is thermally transformed by heating, in the absence of oxygen, into a solid rich in carbon (charcoal) and, simultaneously, into volatile matter (liquids and gases). The solid obtained (called biochar), apart from being a carbon reservoir, can be incorporated into the soil, providing advantages for agricultural production (Shakoor et al., 2021; Simmons et al., 2021). Liquid and gaseous pyrolysis products can be used to generate electricity or as biofuels (Ge et al., 2021).

To improve the valorization of both products (biomass and plastic waste), co-pyrolysis of waste plastics and solid biomass has been studied and significant synergistic effects on product quality have been achieved (Wang et al., 2021). These synergistic effects, to the high hydrogen/carbon (H/C) ratio which, combined with the low oxygen/carbon (O/C) ratio of waste plastics, may be due as they can equilibrate the high O/C ratio and low H/C ratio characteristics of biomass. This compensation effect of the components can lead to an increase in quality and uniformity of the products obtained in that co-pyrolysis. Moreover, Burra and Gupta (2018), with mixtures of plastic and pine wood, demonstrated a significant reduction, in values close to 50 kJ mol^{-1}, in the activation energy of the plastic in the presence of pine wood. They concluded that the decrease in activation energy from the combined chemical interaction resulted, among several reactions with similar activation energies, could be due.

Another study conducted by Singh et al. (2021) investigated the kinetics of co-pyrolysis of corn cobs and PE, showing that co-pyrolysis of corn cobs with PE mixture required approximately 10% less activation energy than pyrolysis of corn cobs alone.

Although synergistic effects on co-pyrolysis only in certain biomass/plastic mixtures have been shown (Navarro et al., 2018), it is possible to state that the study of different biomass/plastic mixtures, especially in the case of waste plastic, would be useful for the proper evaluation of the valorization of these materials. In this sense, both the mixture behavior and its kinetics depend on the mixture material type (initial materials) and on the ratio between them in the mixture being co-pyrolyzed (Wang et al., 2021). Consequently, the availability of a kinetic model of the process for identifying the biomass/plastic associations that can improve the co-pyrolysis of these materials in terms of their kinetic characteristics, as well as the knowledge of the thermal behavior and reactivity of the biomass/plastic mixtures may be helpful in the design and optimization of pyrolytic processes for these materials.

Studies on the thermal reactivity of organic materials using gravimetric techniques have been presented in several publications (Díaz et al., 2021; Xiao et al., 2020). In this respect, thermic analysis (Thermogravimetric Analysis—TGA, Difference Thermogravimetry—DTG and Differential scanning calorimetry—DSC) provides a measurement of the weight loss of the sample as a function of time and under different temperature regimes and the data obtained under different heating rates can be used to determine the thermal degradation kinetics by applying the Arrhenius equation (Díaz et al., 2021).

Volatile organic compounds (VOCs) from the thermal decomposition of polymeric materials have been identified with gas chromatography–mass spectrometry (GC–MS) by several authors. According to Ballice et al. (1998), thermal decomposition of LDPE and HDPE at 300–500 °C ranged straight- and branched-chain paraffins, olefins (C_1–C_{30}) and aromatic hydrocarbons.

The study of both thermal and kinetic behavior during pyrolysis of different biomass/plastic mixtures (*Eucalyptus globulus* with HDPE and LDPE) are the objectives of this study. Additionally, to identify the behavior during pyrolytic degradation, of the main components of biomass (cellulose, hemicellulose, lignin), the mixtures evolution of each component with HDPE and LDPE has been studied.

2. Materials and methods

2.1. Characterization and storage of raw material

Eucalyptus globlulus (EG) branches and twigs with 0.5–5 cm in diameter have been used. These pieces were obtained by trimming EG plants from which leaves and non-wood twigs have been removed prior to grinding in a hammer mill. The materials have been collected from Campus "La Rábida", University of Huelva (Huelva, Spain). This raw material has been prepared in accordance with TAPPI *T* 247 cm-02 (TAPPI Test Method T 257 cm-02, 2012). Portions of the homogenized wood lot have been subjected to quantitative acid hydrolysis with 72% sulfuric acid (TAPPI *T* 249 cm-85) (TAPPI Test Method T 249 cm-85, 1985). The solid residue after hydrolysis was recovered by filtration and considered as Klason lignin. The monosaccharides and acetic acid contained in hydrolyzates were determined by HPLC in order to estimate (after corrections for stoichiometry and sugar decomposition) the contents of samples in cellulose (as glucan) and hemicelluloses (as xylan).

The chemical characterization of EG used in this study and the characterization of the other similar materials by other authors are shown in Table 1.

General-purpose low-density polyethylene (LDPE) grade (LD 605BA, Exxon Mobil). Supplied in powder form with 0.76 g cm^{-3} melt density. HDPE (HD 7957.04 Exxon Mobil), chips of $5 \times 5 \times 2$ mm, have been used. In both cases, LDPE and HDPE, can be considered water and ash free.

2.2. Cellulose, hemicellulose and lignin extraction from Eucalyptus globulus

The raw material was ground and sieved to obtain a uniform chip size. The chips thus obtained were treated with 100 g L^{-1} NaOH concentration under 30 °C and 60 min. Treatments were conducted in 1L beakers that were immersed in a thermostated bath and stirred at 5 min intervals. Once the treatment was finished, the resulting suspension (hemicellulose) was filtered and the solid washed with water and neutralized with 2 *N* acetic acid and dried at room temperature. After drying, the solid was subjected to quantitative acid hydrolysis (72% sulfuric acid) to extract the lignin remaining in the solid. The liquid phase from

Table 1
Average chemical composition for *Eucalyptus globulus* (EG) used and other bibliographic EG composition[a].

	Eucalyptus globulus				
	Present study	Garrote and Parajó (2002)	Leschinsky et al. (2009)	Rencoret et al. (2011)	Miranda et al. (2013)
Ash (%)	0.6 ± 0.1	n.d.	0.4	0.4	12.1
Extractives (%)	2.7 ± 0.08	n.d.	n.d.	0.6–2.2	6.5
Glucan (%)	44.1 ± 2.7	46.3	41.7	46.1	68.4
Klason lignin (%)	21.8 ± 2.0	22.9	22.9	19.8	26.6
Xylan (%)	18.6 ± 1.7	16.6	15.3	17.1	23.2
Arabinan (%)	0.1 ± 0.02	0.2	0.1	0.1	0.2
Galactan (%)	1.3 ± 0.4	1.4	1.7	1.5	1.5
Mannan (%)	1.1 ± 0.4	1.1	1.9	1.2	1.3
Acetyl gr. (%)	3.5 ± 0.2	3.1	3.5	3.3	3.2

[a]Raw material percentages (100 kg dry matter).

the extraction was adjusted to pH 4.5–5.5 with 37% HCl, supplied with 4 volumes of 95% ethanol and centrifuged at 4500 rpm for 3 min. Then, the precipitate formed (cellulose) was washed with 95% ethanol and freeze-dried.

2.3. Mixtures of Eucalyptus Globulus and its fractions with HPDE and LPDE

In order to carry out the study of co-pyrolysis of high and low density polyethylene with *Eucalyptus globulus* biomass and its different fractions, the following mixtures have been proposed:

- *Eucalyptus Globulus* and high density polyethylene: 80% EG–20% HPDE, 60% EG–40% HPDE, 40% EG–60% HPDE and 20% EG–80% HPDE.
- *Eucalyptus Globulus* and low density polyethylene: 80% EG–20% LPDE, 60% EG –40% LPDE, 40% EG–60% LPDE and 20% EG–80% LPDE.
- Main biomass components and high density polyethylene: 40% Cellulose–60% HDPE and 70% Cellulose–30% HDPE; 40% Hemicellulose–60% HDPE and 70% Hemicellulose–30% HDPE; 40% Lignin–60% HDPE and 70% Lignin–30% HDPE.
- Main biomass components and low density polyethylene: 40% Cellulose–60% LDPE and 70% Cellulose–30% LDPE; 40% Hemicellulose–60% LDPE and 70% Hemicellulose–30% LDPE; 40% Lignin–60% LDPE and 70% Lignin–30% LDPE.

For the previous mixtures, the size of the different components was homogenized to a size of approximately 0.5–5 cm. Completely uniform mixtures were obtained, using a weight %.

2.4. Pyrolysis and TGA experiments

Thermo-gravimetric analyzer (TGA, DSC) (Mettler Toledo TGA/DSC1 STARe System) to verify the thermo-chemical decomposition behavior has been used. The TGA experiments were performed by heating a 50–130 mg sample from 25 °C to 800 °C at four heating rates of 5, 10, 15 and 20 °C min^{-1}, respectively, under a nitrogen flow of 20 cm^3 min^{-1}. TGA data were analyzed to determine the Arrhenius Activation Energy (Ea) and the Pre-exponential Constant (A) using ASTM-E1641-16 and ASTM E2890-12 standard methods.

2.5. Kinetic study

ASTM-E1641-16 standard method is an isoconversional model (in which at a fixed degree of conversion, the reaction rate is a function of temperature only) based on the calculation of the dependence of the effective Activation Energy on the conversion degree achieved at a given temperature. This dependence is used to calculate the kinetic constants without prior knowledge of the mechanism of thermal processes. The main assumption of the method is that the function modeling the degree of conversion does not change under different heating rates. Therefore, measurements at different heating rates are necessary (at least 3).

ASTM-E1641 is based on the Arrhenius kinetic equation and provides a fast calculation of the kinetic parameters very useful in complex reactions involving multiple processes. In this sense, both Arrhenius Activation Energy (Ea) and pre-exponential factor (A) by thermogravimetry, based on the assumption that the decomposition is first-order kinetics using the Ozawa/Flynn/Wall isoconversional method (Junmeng and Siyu, 2009; Ozawa, 1965; Vimalathithan et al., 2019).

$$\frac{d\alpha}{dt} = \frac{A}{\beta} e^{-\frac{E}{RT}} f(\alpha) \tag{1}$$

Where: α is the value related to a given conversion degree, t is time, β the heating rate, A is the Arrhenius pre-exponential factor, T is temperature, E the Activation Energy at a given value of conversion rate, R the gas constant and $f(\alpha)$ is the differential conversion function.

For each given value of α, in the above equation, Eq. (1) can be rearranged (Eq. (2)). In this equation, the subscript α indicates the degree of conversion achieved.

$$\frac{d \ln\left(\beta \frac{d\alpha}{dt}\right)}{d\left(\frac{1}{T}\right)} = -\frac{E_\alpha}{R} \tag{2}$$

Therefore, Eq. (3) proceeds from reordering Eq. (2).

$$\ln\left(\beta \frac{d\alpha}{dT}\right)_\alpha = \text{constant} - \frac{E_\alpha}{R} \tag{3}$$

The previous equation for non-isothermal processes could be described by the following equation (Leng and Huang, 2018; Mishra and Mohanty, 2018).

$$\ln(\beta_i) = \ln\left(\frac{A_\alpha E_\alpha}{R g(\alpha)}\right) - 5.331 - 1.052 \frac{E_\alpha}{R T_{\alpha,i}} \tag{4}$$

Where: β the heating rate, A is the Arrhenius pre-exponential factor and $g(\alpha)$ is the reaction model. Thus, the above equation, for each known α, can be transformed into Eq. (5).

$$\ln(\beta) = \ln\left(\frac{A_\alpha E_\alpha}{R}\right) - \ln g(\alpha) - 0.4567 \frac{E_\alpha}{RT} \tag{5}$$

Therefore, a function between temperature T and reaction rate (thermal degradation of organic matter) d/dt for each degree of conversion and under different heating rates, the Activation Energy, when plotting $\ln(\beta)$ versus $1/T$, a simple linear equation could be plotted. In that form, a straight line with a slope of –0.4567 Ea/R was obtained and Ea could be deduced. Furthermore, A from the intercept with the axes, can be calculated.

Netzsch Kinetics Neo (v2.1.2.1) software was used to determine Ea and pre-exponential factor (A) by using ASTM-E698-11. The software used, due to both three replicates used and the strict thermokinetic criteria introduced, provides data with a high determination coefficient ($R^2 > 0.95$) for all of the exposed data. Thus, a statistically robust result can be offered for both measured parameters (Ea, A).

2.6. Gas chromatography analysis

Gas samples from the pyrolysis process in the temperature ranges of maximum degradation of EG, HDPE, LDPE and EG-HDPE, EG-LDPE mixtures obtained at the exit of the TGA (heating rate: 20 °C min^{-1}; N_2 flow: 20 cm^3 min^{-1}) were collected in fritted glass TD tubes (Supelco, Bellefonte, PA; O.D.: 6.35 mm; length: 88.9 mm) for 1.5 min. Tubes contained 100 mg of Tenax® TA (80–100 mesh purchased from Supelco, Bellefonte, PA) packed in layers of silanized glass wool.

After sampling, TD–GC–MS analysis was performed using a thermal desorption system unit (TD-20, Shimadzu, Japan) coupled to the GC–MS/MS system (GCMSQP8030 Ultra System, Shimadzu, Japan) fitted with a HP-5 MS column (60 m, 0.25 mm I.D. 0.25μm film thickness, J&W Scientific, Agilent Technologies, USA). Volatile organic compounds (VOCs) were desorbed at 280 °C for 10 min, preconcentrated in the cold trap at −16 °C and then thermally desorbed at 280 °C for 8 min. The column was kept at 60 °C for 7 min, ramped at 8 °C min^{-1} to 280 °C, held for 4 min. Helium, at constant flow rate of 1.3 mL min^{-1}, was used as the carrier gas. The temperatures of the transfer line and ion source were maintained at 280 and 230 °C, respectively. The mass spectrometer was operated in scan mode (42–450 m z^{-1}). VOCs compounds have been identified by comparison of the mass spectra with those in the database of NIST11 library. For control and data analysis, GC–MS Postrun Analysis Shimadzu was used. The MS was turned with perfluorotributylamine (PFTBA).

3. Results and discussion

3.1. Characteristics of raw materials (EG, HDPE, LDPE)

Thermograms of both mass loss (TGA) and their derivative (DTG with respect to time corresponding to pyrolytic decomposition of EG, HDPE and LDPE, at 20 °C min^{-1}, under nitrogen atmosphere, are shown in Fig. 1 (for kinetic parameters calculation, four thermograms have been carried out at four heating rates 5, 10, 15 and 20 °C min^{-1}, for illustration purposes only the last thermogram has been shown in figures. The remaining data in the additional data have been added). In this form, Fig. 1a, the mass loss profile of EG obtained by thermogravimetric analysis and Figs. 1b and 1c are HDPE and LDPE profiles, respectively.

In Fig. 1a, a characteristic thermal degradation (Barneto et al., 2011) is shown. TGA curve presents three different regions, so that it is a combination of the thermal degradation of the major components of lignocellulosic material, i.e. hemicellulose, cellulose and lignin degradation (Barneto et al., 2011). In this form, Fig. 1a shows the three regions corresponding to interstitial water loss (27–160 °C) (Domínguez et al., 2017), active pyrolysis zone (160–430 °C) and passive pyrolysis zone (430–500 °C). The most active pyrolysis process starts at about 250 °C with its maximum degradation rate at 310 °C. In this second degradation, the main degradation (main peak of the DTG curve) corresponds to hemicellulose and part of cellulose degradation, because some overlap in these components degradation, have been described (Dantas et al., 2013; Lei et al., 2019). Subsequently, the degradation rate for weight loss decreases progressively and, after this, a very low degradation until final temperature could be observed.

In the third region, a small shoulder, which could be related to a higher volatilization of lignin can be observed. In this sense, that lignin decomposes slowly within a temperature range of 180–850 °C has previously been demonstrated (Van de Velden et al., 2010; Yang et al., 2007). Moreover, different compounds volatilization (characterized as extracts) has also been described within this range (Barneto et al., 2011) and other small peaks corresponding to higher temperature regions to the coke formed degradation, in conjunction with a corresponding lignin degradation, can be attributed (Vuthaluru, 2004).

Figures 1b and 1c show TGA and DTG curves obtained from the pyrolytic degradation of HDPE and LDPE respectively, both under a heating rate of 20 °C min^{-1}. TGA and DTG curves clearly show that a main degradation region for HDPE pyrolytic degradation has been found in Fig. 1b. This reaction started at approximately 400 °C with a maximum degradation rate at 490 °C. The values found agree with the available literature (Al-Yaari and Dubdub, 2020; Rodríguez-Luna et al., 2021). However, in Fig. 1c, corresponding to LDPE, a single-stage decomposition profile, mainly within the 400–500 °C, is shown. In this regard, several references indicate that pyrolytic degradation of both low and high density polyethylene in a single step can be modeled(Conesa et al., 1997; Duque et al., 2020).

3.2. Thermal behavior of EG, HDPE and LDPE mixtures

Figs. 2 and 3 show data found in TGA and DSC at 20 °C min^{-1} for EG–HDPE and EG–LDPE mixtures, respectively.

From Fig. 2, that EG–HDPE decomposition occurs in two main stages can be stated: The first phase corresponds to the joint loss of hemicellulose, cellulose and HDPE. This phase begins at 200 °C and extends up to 400 °C. In this sense, it can be seen that the maximum degradation, which for EG 80%–HDPE 20% mixture is at 316 °C, progressively decreases to 284 °C for EG 20%–HDPE 80% mixture. The second phase, which overlaps with the others, is due to the slow decomposition of lignin, which extends from low temperatures up to 500 °C (Cheng et al., 2012). It should be noted that most of the organic matter degrades at temperatures between 200–400 °C. Therefore, this is the most significant phase of the process and is one that results in the highest release of gaseous products. The amount of non-degraded material generated at 800 °C also varies according to the relative amounts of EG and HDPE, varying between 20.8% for EG 80%–HDPE 20% and 1.6% for EG 20%–HDPE 80%.

Fig. 3, on the other hand, shows, in all EG–LDPE ratios, two distinct peaks due to the temperature difference between the degradation of hemicellulose–cellulose and that corresponding to LDPE. From Fig. 3, therefore, it can be deduced that EG–LDPE decomposition takes place in two main stages: The first stage corresponds to hemicellulose–cellulose joint losses. This stage began at 200 °C and was extended up to 350 °C. The peak in the DSC figure corresponding to hemicellulose–cellulose becomes lower as the relative amount of EG to LDPE decreases. The second stage, which is found between 300–500 °C, to LDPE decomposition is due. Although, in contrast to that found for EG–HDPE mixtures, displacement of the maximum degradation EG–LDPE mixtures can be observed in these mixtures. Thus, the temperature of the maximum degradation peak for EG 80%–LDPE 20% mixture is at 421 °C and progressively increases to 470 °C for EG 20%–LDPE 80% mixture. The amount of non–degraded material produced at 800 °C also varies depending on the relative amounts of EG and LDPE, ranging from 7.3% for EG 80%–LDPE 20% mixture to 3.4% for EG 20%–LDPE 80% mixture.

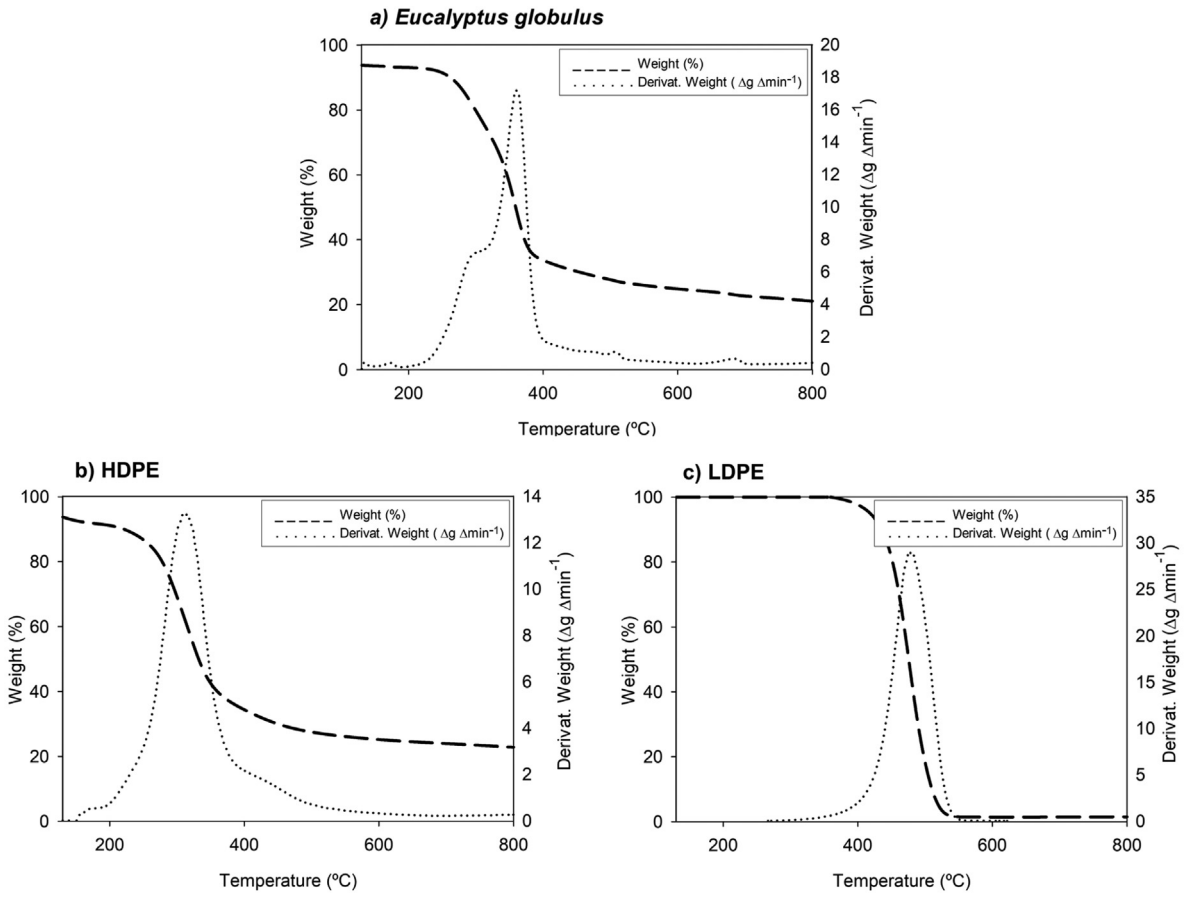

Fig. 1. Thermogravimetric data (TGA) (%) and Derivative Thermogravimetric data (DTG) (g min^{-1}) during the pyrolysis of *Eucalyptus globulus* (EG, a), High Density Polyethylene (HDPE, b) and Low Density Polyethylene (LDPE, c) at 20 °C min^{-1}.

3.3. Kinetic behavior of raw materials and mixtures

Ea and A by the ASTM-E1641 method (Eq. (5)) has been calculated. The maximum temperatures from TGA data have been obtained. As was discussed in Section 2.4, the FWO method allows obtaining the kinetic parameters from a plot of the natural logarithm of the heating rates, $\ln(\beta i)$, versus $1000/T_{\alpha,i}$. These plots represent a linear correlation at the conversion value $\alpha = 0.05$ higher than 0.95 in all cases.

In Fig. 4, the evolution of the Activation Energy and the pre-exponential factor in the mixtures under study for both EG–HDPE (Fig. 4a) and EG–LDPE (Fig. 4b) are shown. Accordingly, the values corresponding to 0% have been referenced to *Eucalyptus globulus* as raw material and, progressively, increases the percentage of polyethylene up to 100% in which the values of HDPE or LDPE as raw material have been related. Thus, associated values to 0% of polyethylene are the calculated values for 100% of pure EG. At the other extreme of both graphs, the values of 100% for each polyethylene correspond to the values calculated for pure HDPE and LDPE, respectively.

The Activation Energy value obtained for EG is 154 kJ mol^{-1}. The calculated value was in the same range as those found by other authors for several eucalyptus varieties. In this sense, Poletto et al. (2012) found 208 kJ mol^{-1} in *Eucalyptus grandis*, da Silva et al. (2017) found 140.46 kJ mol^{-1} in *Eucalyptus dunnii* and Cheng et al. (2017) found among 117–155.8 kJ mol^{-1} in several eucalyptus residues. Alternatively, the calculated Activation Energy value is 206 kJ mol^{-1} for HDPE and 173 kJ mol^{-1} for LDPE.

Among them, the difference in Activation Energy between different types of polyethylene at different chain branches, which altered the distribution of chemical bonds, morphologies and orientation structures between the two polyethylene raw materials may be related. In this sense, it has been demonstrated that these differences in structure imply different values in their physical characteristics (Zhang et al., 2004).

For these materials, the Ea values obtained are consistent with the range of values found by some other authors. In this respect, for HDPE, Khalturinskii (1987) calculated 146.5 kJ mol^{-1}, Sinfrônio et al. (2005) estimated 204–269 kJ mol^{-1} and Aboulkas et al. (2010) found 215–221 kJ mol^{-1}. Additionally, for LDPE, Saha and Ghoshal (2007) determined 190 kJ mol^{-1} and Aboulkas et al. (2010) found 179–188 kJ mol^{-1}.

According to the results obtained by Zhou et al. (2006) and the adequate correlation coefficients ($R^2 > 0.9$ in all cases) obtained in the calculation of the kinetic analysis, that the first-order reactions can explain quite satisfactorily the different weight loss sub-intervals found for the materials and their mixtures. Thus, the pyrolysis process of both the original materials and the EG–HDPE and EG–LDPE mixtures by using a first-order reaction can be described. Therefore, the experimental results calculated using ASTM-E1641, for the pure products, indicate that the model can satisfactorily describe the complexity of the pyrolysis process of the tested products.

In Fig. 4a a decrease in both Activation Energy and pre-exponential factor at low amounts (20%) of HDPE has been found. Similar synergistic effects have been previously found by other authors in different biomass–plastic mixtures (Alam et al., 2020; Oyedun et al., 2014). According to exposed conclusions by Zhang et al. (2016) and Burra and Gupta (2018), the decrease in the Activation Energy to an overlap among different degradation reactions, with similar energies, could have a synergistic effect able

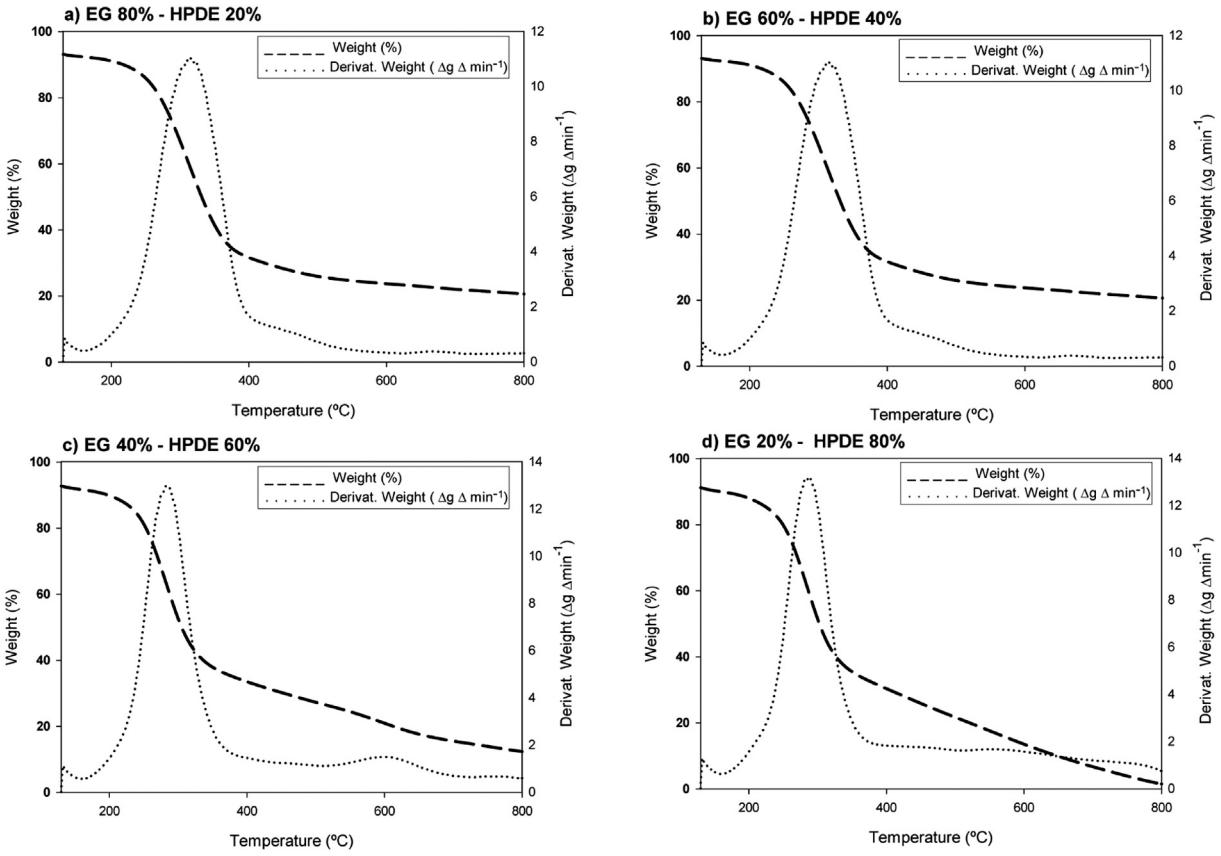

Fig. 2. Thermogravimetric data (TGA) (%) and Derivative Thermogravimetric data (DTG) (g min^{-1}) during the pyrolysis of *Eucalyptus globulus* – High Density Polyethylene (EG–HDPE) mixtures at 20 °C min^{-1}.

to cause the reduction of the Activation Energy of the mixture and, hence, accelerates the kinetics of the pyrolysis process. Other authors, to adequate hydrogenation produced by the constituent compounds of plastic (Chen et al., 2020), attribute this synergistic effect in kinetic values. Xue et al. (2015) indicated that a synergy may arise from the interaction between hydrogen in polymer and oxygenated compounds in biomass, which may facilitate the breaking of the C–C bonds in polymer.

However, Hassan et al. (2020) and Mishra et al. (2019) found different positive and negative effects on the synergistic effect of activation energies and pre-exponential factor in different biomass–plastic mixtures. In our study, after the minimum in kinetic values, different values, for both Ea and A, calculated for each mixture, are similar to the algebraic sums of those of each separate component (EG and HDPE). Therefore, the exposed synergistic effect was not verified in the other mixtures.

An effect similar to that found in Fig. 4a (EG–HPPE mixtures), in EG–LDPE mixtures (Fig. 4b) has been found, in this case, minimum values for both Ea and A at 40% LDPE have been calculated. Thermal decomposition of synthetic polymers by free radical chain reaction mechanism has been described for the pyrolysis of hydrocarbons and biomass char (Willems and Froment, 2002). Thus, the initial reactions, as homolytic bond breaking processes, have been described by different authors (Aboulkas et al., 2010). These elementary reactions give rise to propagation reactions, and radical recombination (Aboulkas et al., 2010) which is found to be more efficient for HDPE than for LDPE due to the very different spatial structure between the two types of polyethylene. Dou et al. (2007) demonstrated, in the pyrolysis of plastic materials, limiting mechanisms in degradation reactions, since these are mainly surface reactions, are given by diffusion mechanisms. In the case of pyrolysis involving biomass and plastic, which is a heterogeneous reaction, radical diffusion mechanisms may be much stronger than those concerning the energetics.

Optimal biomass plastic ratio values found are similar to those reported by other authors as optimal for an efficient pyrolysis. Among these were Kai et al. (2019) who found a 20:80 HDPE:Corn stalk mixture as optimal, Hassan et al. (2020) utilized a 60:40 HDPE:Sugarcane bagasse mixture and Alam et al. (2020) used a 75:50 LDPE:Bamboo sawdust mixture.

3.4. Thermodynamic behavior of mixtures pyrolysis degradation

In Fig. 5, variations of Enthalpy (ΔH) and Gibbs free energy (ΔG) for the studied mixtures pyrolysis are shown. Enthalpy variation as the amount of energy exchanged in a chemical reaction is defined. It involves the difference in enthalpy between the reactant and the activated complex (Ruvolo-Filho and Curti, 2006).

In this study, for the kinetic method selected ($\alpha = 0.05$), minimum enthalpy values (Fig. 5a) are observed for a percentage of 20 (20% EG–80% HDPE) in the case of HDPE and close to 40 (40% EG–60% LDPE) for LDPE, similar to that found for Activation Energy, which presents an analogous variation. Minor differences are observed between Activation Energy and enthalpy values, which indicates the feasibility of reactions under the exposed conditions due to the low energy level to be overcome once the activated complex has been reached.

Variation in Gibbs free energy (Fig. 5b) reflects energetic increase in the reaction system during the approach of the reactants and formation of the activated complex. It also shows the stability of its thermodynamic equilibrium. The difference among obtained values reaches maximums 31 and 37 kJ mol^{-1} for samples with LDPE and HDPE, respectively. In case of HDPE the lowest values

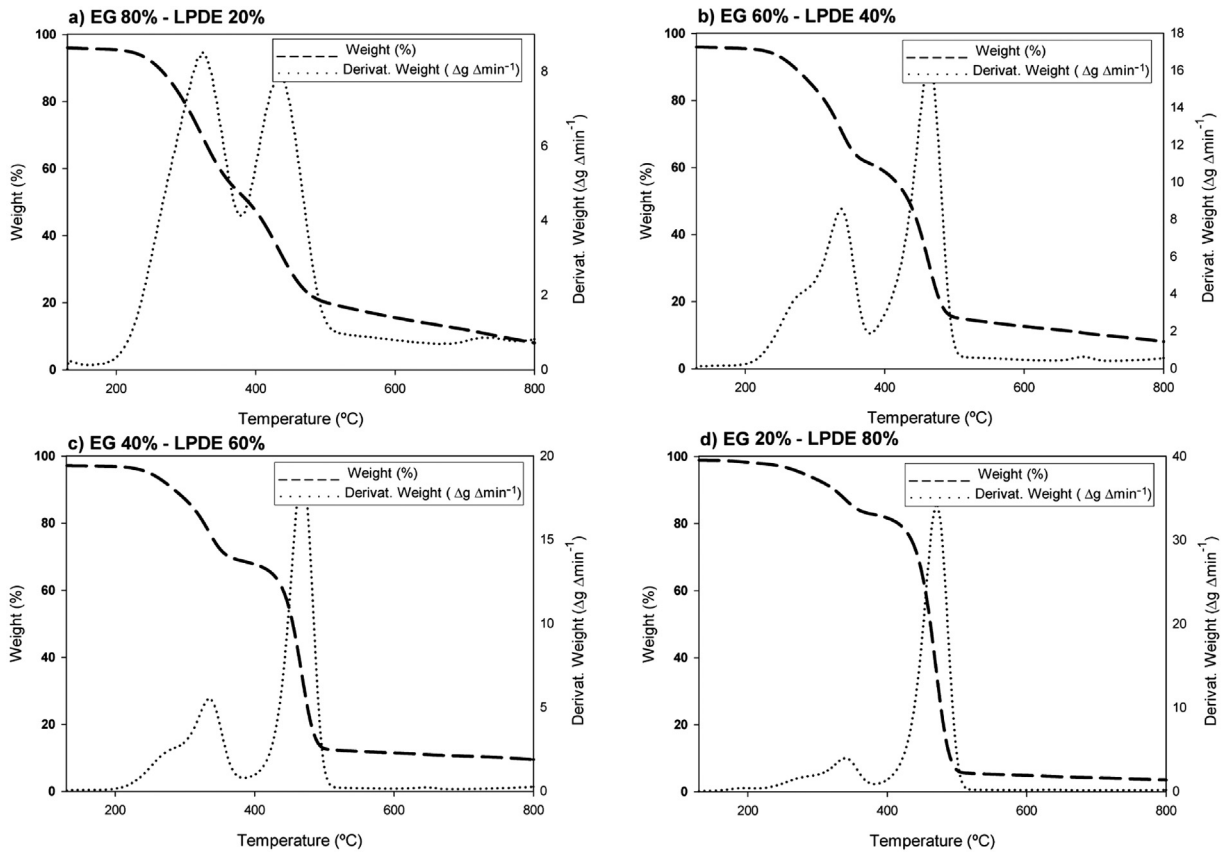

Fig. 3. Thermogravimetric data (TGA) (%) and Derivative Thermogravimetric data (DTG) (g min^{-1}) during the pyrolysis of *Eucalyptus globulus* – Low Density Polyethylene (EG–LDPE) mixtures at 20 °C min^{-1}.

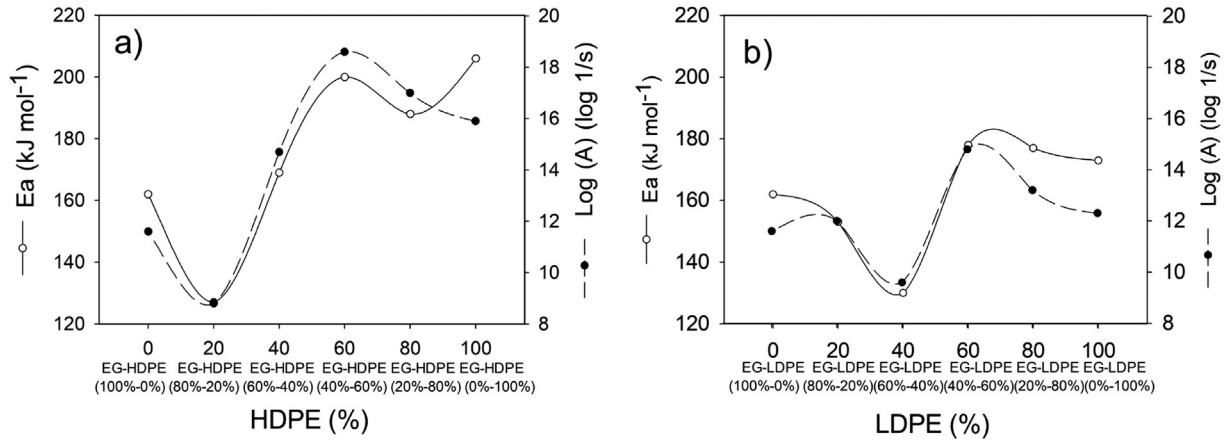

Fig. 4. Pyrolysis Activation Energy (Ea) and Arrhenius Pre-exponential factor (as Log A) evolution calculated for *Eucalyptus globulus*–High Density Polyethylene (EG–HDPE, (a) and *Eucalyptus* globulus–Low Density Polyethylene (EG–LDPE, (b) mixtures.

are in the range of 40 to 80% polyethylene, for LDPE the minimum value at 60% polyethylene is found. Similar values to that found in this study for other raw materials such as rice straw (Xu and Chen, 2013) have been obtained, although they are lower than the values found by other authors in mixtures of biomass and plastics (Mumbach et al., 2019; Pradhan et al., 2020).

3.5. Eucalyptus globulus main components (cellulose, hemicellulose and lignin) with HDPE, LDPE mixtures: thermal behavior

The biomass composition principally involves cellulose, lignin and hemicellulose in variable proportions. Thermal degradation of individual components involves changes in Ea during the process since different components will be degraded depending on the degradation temperature of each compound. To investigate kinetic parameter variations and the relative influence of these components in the mixtures, thermogravimetric and kinetic studies with cellulose, hemicellulose and lignin for both HDPE and LDPE have been performed. The biomass components used in this study from the selective separation of these components from EG as raw material have been obtained.

As shown in Fig. 6a, the pyrolytic degradation of cellulose is in a narrow temperature range (290–380 °C). This region is where most of the total mass loss of the process is found because of

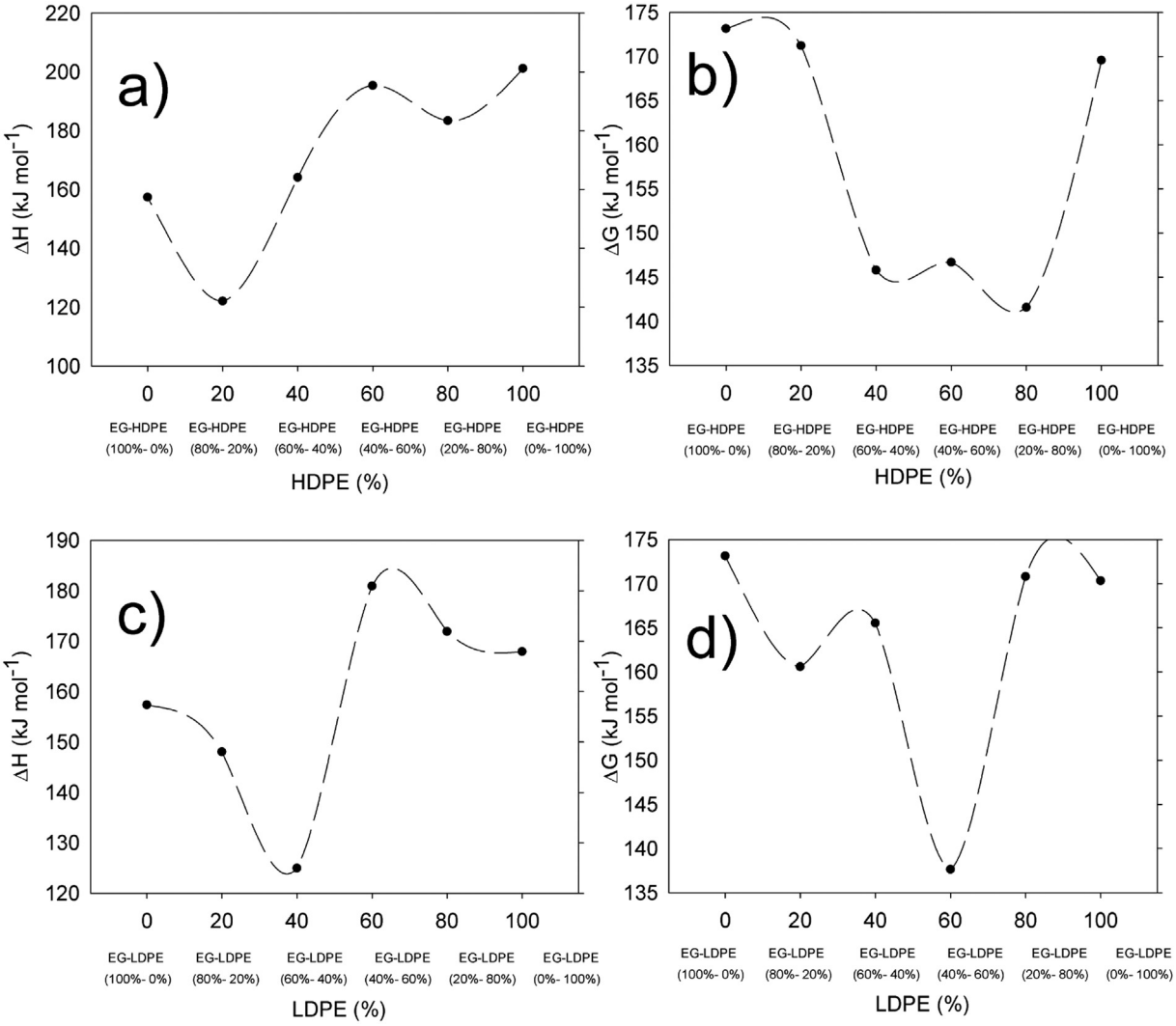

Fig. 5. Variation of enthalpy of formation (ΔH) and Gibbs free energy (ΔG), in pyrolysis degradation, calculated for *Eucalyptus globulus*–High Density Polyethylene (EG–HDPE) and *Eucalyptus globulus*–Low Density Polyethylene (EG–LDPE) mixtures.

strong devolatilization with a peak in the DTG plot. The maximum rate of weight loss occurs at 358 °C. After this region, weight loss is slow due to the decomposition of the carbonaceous material contained in char residue (Yeo et al., 2019). Generally, only a single peak has been observed, indicating that single-stage thermal decomposition of the cellulose pyrolysis has been observed. The solid residue obtained at 800 °C is 6.7%. In this sense, because cellulose is formed by a glucose polymer, with a well-ordered structure, high thermal stability to cellulose is resulted.

Fig. 6b, the pyrolytic degradation of hemicellulose is shown. In contrast, to cellulose structure, hemicelluloses have an irregular structure and, therefore, a more amorphous and aleatory structure, which results in a lower degradation temperature of hemicelluloses compared to cellulose. This figure shows an initial dehydration stage followed by two degradation peaks (237 and 271 °C) representing a two-stage devolatilization process of the hemicellulose content. The chemical composition of the analyzed cellulose is shown in Table 1. In this form, according to Fig. 6b, hemicelluloses initiated its thermal decomposition at 207 °C reaching up to 460 °C. In this process, based on both TGA and DTG profiles, several process steps can be observed. It begins with the water loss phase (up to 150 °C). From 207 °C onward, where most of the mass is lost, and where the decarboxylation and decarbonylation reactions are found (Cheng et al., 2012). Two peaks are observed at this stage. The first peak to the decomposition of the side chain structure is attributed, whereas, the second peak to the fragmentation of other previously depolymerized units is also attributed (Shen et al., 2010). In this regard, according to Dussan et al. (2017) (pentoses follow different reactive pathways than hexoses. In this sense, it has been shown that xylose and arabinose degradation occurs at lower temperatures than mannose, glucose and galactose (Shukry et al., 1991). Finally, a stage in which the decomposition of hemicellulose into carbon occurs from 320 °C (Cheng et al., 2017).

In Fig. 6c the pyrolytic decomposition of lignin is shown. According to the results shown by Cheng et al. (2012), both the decomposition profile (TGA, DTG) and the kinetic parameters depend on both the type of starting material and the technology used in extraction and isolation. In that figure, it is observed that lignin decomposes over a wide range of temperatures, from ambient to about 800 °C. In this respect, Yeo et al. (2019) had demonstrated that because of its numerous ether bonds, hydroxyl groups, methoxy, etc., lignin is the most difficult biomass component to degrade due to its complex structure. In Fig. 6c the typical stages of lignin pyrolysis are shown. Initially, at the temperature range of 150–250 °C melting of lignin and release of the weakly bonded functional groups is produced (Galano et al., 2017). The next stage (300–550 °C) involves the breakdown of the β–O–4

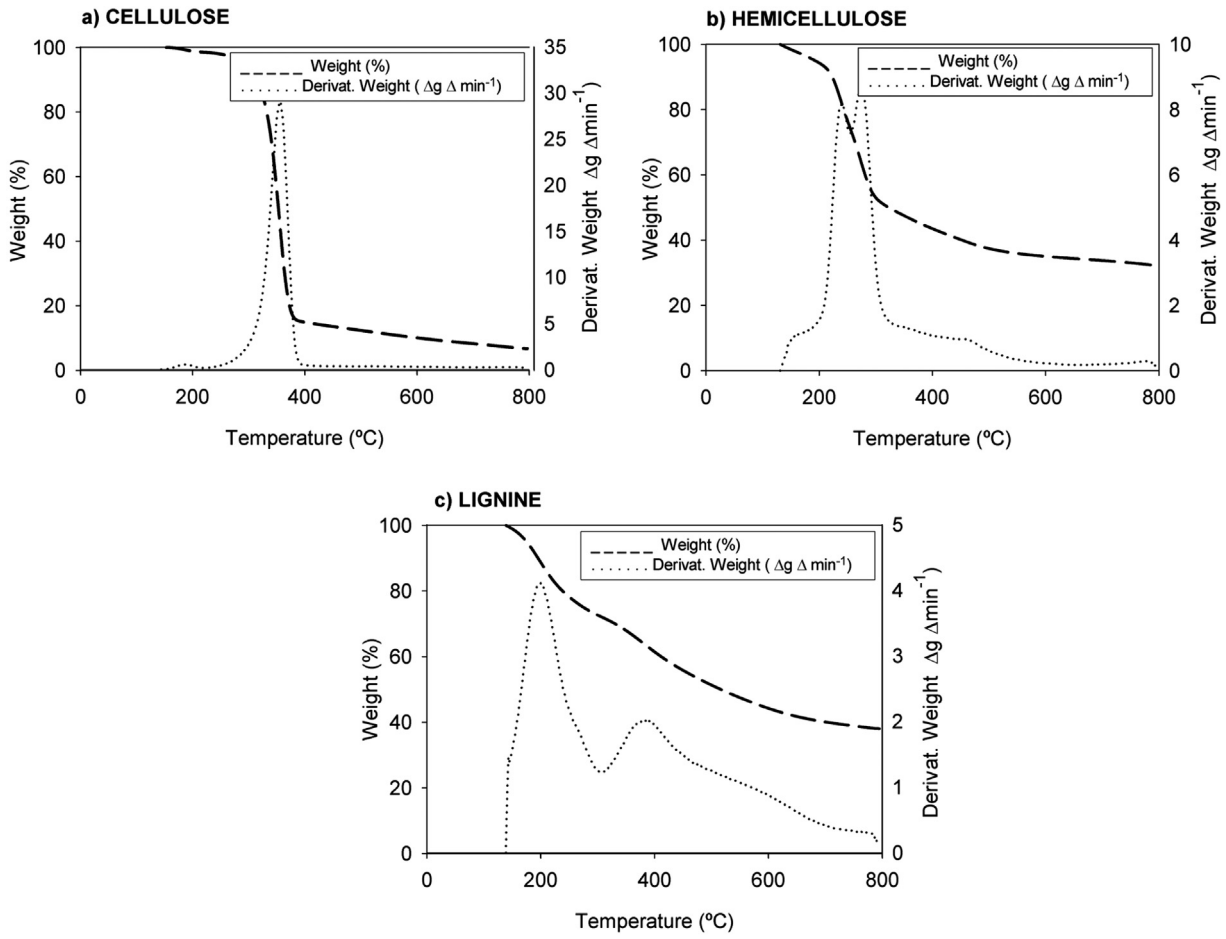

Fig. 6. Thermogravimetric data (TGA) (%) and Derivative Thermogravimetric data (DTG) (g min^{-1}) during the pyrolysis of Cellulose (a), Hemicellulose (b) and Lignin (c) obtained from *Eucalyptus globulus* at 20 °C min^{-1}.

bonds (Lu et al., 2021). This is followed by the secondary pyrolysis reaction (550–800 °C) in which several types of bonds are broken simultaneously (Lu et al., 2021). The solid residue remaining from the pyrolysis of lignin (39.0%) is higher than that obtained in cellulose and hemicellulose pyrolysis. This high solid content to the complex structural network with high thermal stability of these compounds can be attributed (Yeo et al., 2019).

To evaluate the influence of the quantities of polyethylene on each major components of the biomass (cellulose, hemicellulose, lignin), different ratios of these components with HDPE and LDPE have been performed. The ratios evaluated are cellulose (40%)–HDPE (60%) and cellulose (70%)–HDPE (30%) and, on the other hand, cellulose (40%)–LDPE (60%) and cellulose (70%)–LDPE (30%) also with hemicellulose and lignin have been tested.

In Figs. 7 and 8, the TGA and DTG profiles of the tested mixtures for HDPE and LDPE respectively are shown.

In this form, in Fig. 7a, cellulose decomposed between 250–300 °C, while HDPE decomposed at higher temperatures of 400–500 °C have been observed. The cellulose and HDPE mixture had two stages of mass loss in temperature range corresponding to the decomposition of cellulose (250–300 °C) and HDPE (400–500 °C) respectively. This fact is more clearly in Fig. 7b can be observed. Here, due to the higher percentage of cellulose in the sample (70%), higher is the associated curve, in the graph corresponding to DTG, for cellulose. The DTG curve peaks corresponding to both cellulose decomposition and HDPE were similar, although located at lower temperatures than those obtained for cellulose (Fig. 7a) and similar to those found for HDPE (Fig. 7b) have been observed. The lower temperature found for cellulose degradation could have been due to the interaction between biomass carbon and HDPE (Chattopadhyay et al., 2016). Similar effects to those found have been previously described by Wang et al. (2021). Also, Yuan et al. (2018) investigated the synergistic effects during co-pyrolysis of cellulose and HDPE. Their results showed that mixtures of these components indicate that, due to hydrogen transfer from HDPE chain breakage, cellulose decomposition can be enhanced.

Similarly, a similar effect to that observed for cellulose–HDPE mixtures, in cellulose–LDPE mixtures (Figs. 8a and 8b) can also be seen. Although, two degradation maxima peak can be observed in these figures. This divergence in degradation maxima to the difference in pyrolytic degradation temperatures between cellulose and LDPE can be attributed.

Also in Fig. 7c, a single degradation between 200–400 °C, with a peak at 303 °C can be obtained, although in Fig. 7d. corresponding to the 70% hemicellulose–30% HDPE, due to the higher proportion in hemicellulose a shoulder at 311 °C and a maximum degradation at 373 °C can be detected. In this sense, a decrease in temperature for the maximum degradation has been observed.

For the hemicellulose–LDPE mixtures (Figs. 8c and 8d) also only one peak of maximum degradation has been observed. In these cases, the maxima correspond to 471 °C for the 40% hemicellulose–60% LDPE mixture and 476 °C for the 70% hemicellulose–30% LDPE blend, so also the increase in the relative amount of LDPE also causes a slight decrease in the temperature for the maximum pyrolytic degradation.

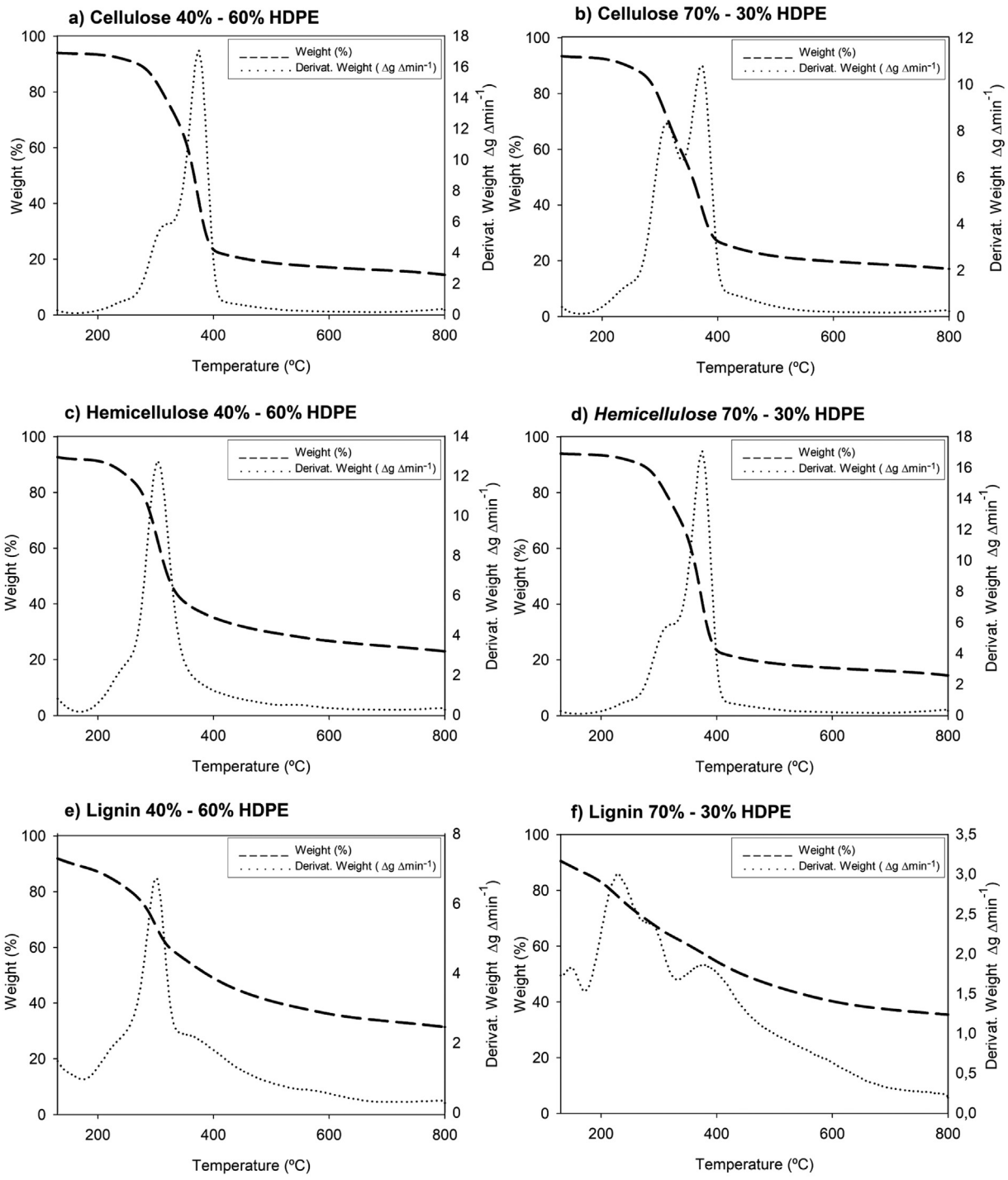

Fig. 7. Thermogravimetric data (TGA) (%) and Derivative Thermogravimetric data (DTG) (g min^{-1}) during the pyrolysis for Cellulose–HDPE mixtures (a, b), Hemicellulose–HDPE mixtures (c, d) and Lignin–HDPE mixtures (e, f) at 20 °C min^{-1}.

As observed in Fig. 7e, HDPE degradation around 255 °C (with a peak at 302 °C) for 40% lignin–60% HDPE mixture and 185 °C (with a peak at 227 °C) for 70% lignin–30% HDPE mixture could be observed. Thus, a greater synergistic effect between HDPE and lignin, with respect to the other components, on the variation of the degradation temperature can be appreciated. According to the Patil et al. (2018) observations, the relatively lower hydrogen content of lignin molecules (H/C_{eff} molar ratio < 0.3), which compensates higher hydrogen content of HDPE, leads to increased synergistic effects in the pyrolytic process of both compounds. In this study, the plastics presumably donate hydrogen during co-pyrolysis, which aids in the depolymerization of lignin. Additionally, since the range of lignin and HDPE decomposition are similar, in the range 170–350 °C an overlap of both degradation regions can be observed and the peaks exhibited are the result of the overlap of lignin and HDPE degradation. Furthermore, in Figs. 7e and 7f, that lignin–HDPE and LDPE mixtures have two regions of thermal degradation, around 155–350 °C and 350–700 °C have been found. The first region is characterized by the breakdown of HDPE and the second by the degradation of

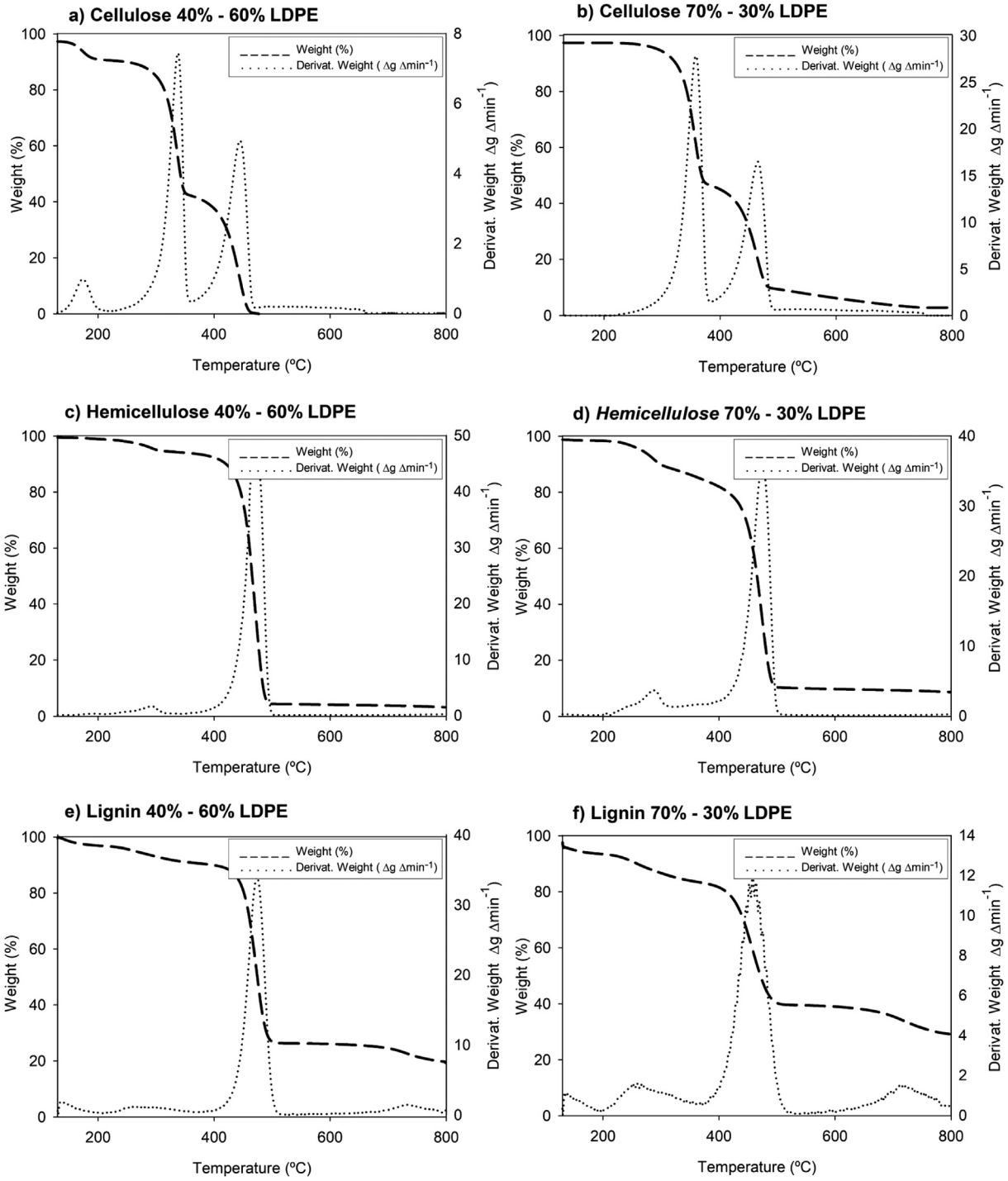

Fig. 8. Thermogravimetric data (TGA) (%) and Derivative Thermogravimetric data (DTG) (g min^{-1}) during the pyrolysis for Cellulose–LDPE mixtures (a, b), Hemicellulose–LDPE mixtures (c, d) and Lignin–LDPE mixtures (e, f) at 20 °C min^{-1}.

remaining lignin, where degradation is more significant in the sample with higher lignin content (Fig. 7f). Overall, it can be seen from the DTG curves that lignin degrades slowly, although its degradation started earlier together with HDPE. HDPE, however, was rapidly degraded. Alternatively, the generated residues from lignin and HDPE mixtures (32%–35%) are higher than those found in HDPE with cellulose and hemicellulose mixtures.

Similarly, to the synergistic effects found for cellulose and hemicellulose with HDPE, for lignin–LDPE mixtures (Figs. 8e and 8f) have also been found.

3.6. Eucalyptus globulus main components (cellulose, hemicellulose and lignin) with HDPE, LDPE mixtures: kinetic behavior

In Fig. 9, the evolution of both Ea and A as a function of the relative amounts of both HDPE and LDPE for cellulose, hemicellulose and lignin are shown. In these figures, the values corresponding to 100% cellulose (Figs. 9a and 9d), hemicellulose (Figs. 9b and 9e) or lignin (Figs. 9c and 9f), to the values of the Activation Energies or Arrhenius pre-exponential factor for the pure compounds are

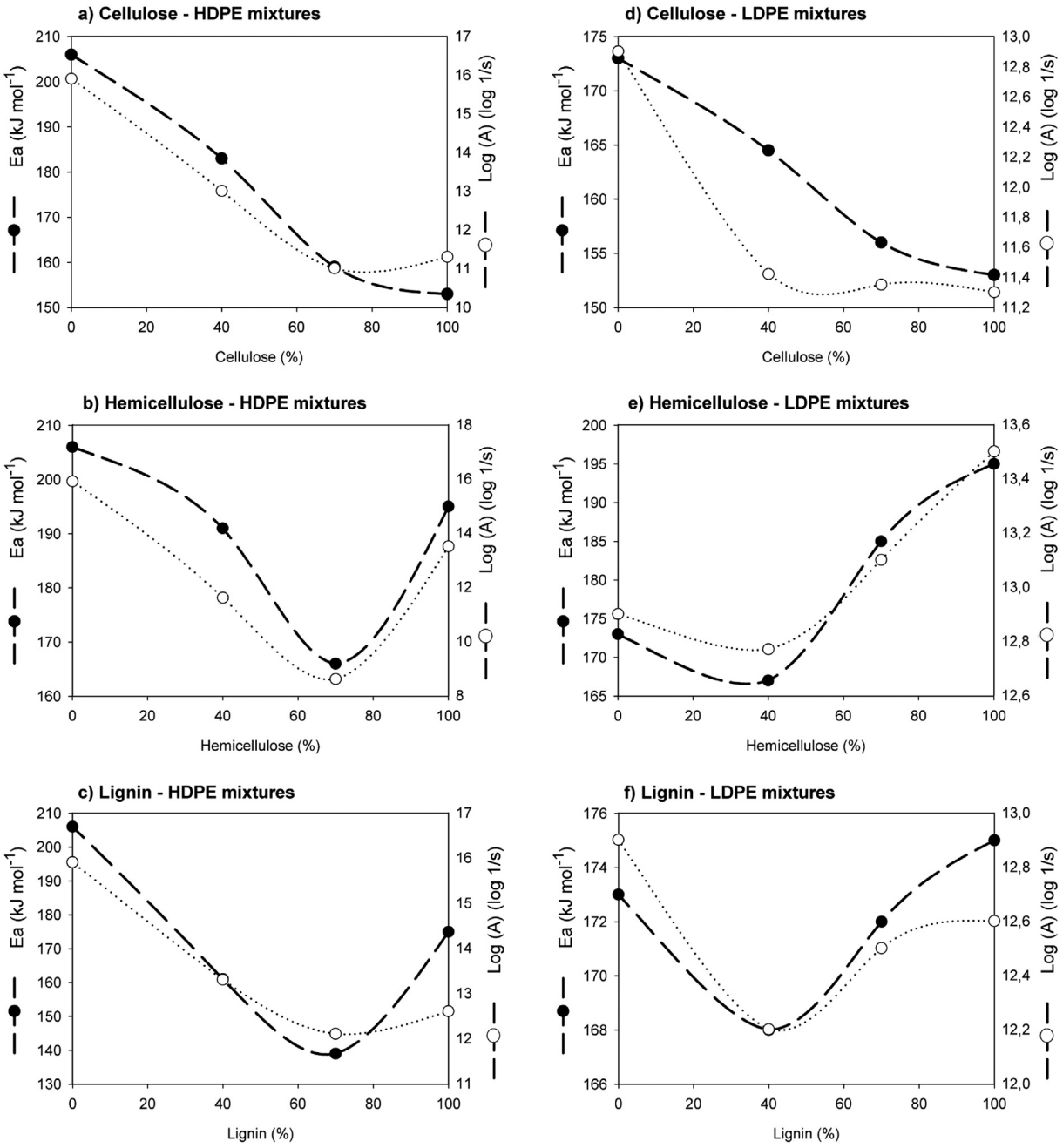

Fig. 9. Activation Energy (Ea) and Arrhenius Pre-exponential factor (as Log A) evolution, in pyrolysis, calculated for the three main components and both studied polyethylenes.

attributed. On the other hand, the values corresponding to 0% of each component are the value of HDPE (Fig. 9a–c) or LDPE (Fig. 9d–f) respectively.

In this regard, the calculated values for the activation energies of the individual components are 153 kJ mol^{-1} for cellulose, 195 kJ mol^{-1} for hemicellulose and 175 kJ mol^{-1} for lignin. These data are within the values found by Lin et al. (2009), Cheng et al. (2012), Quan et al. (2016) and Yeo et al. (2019) for which the Ea found for pyrolysis of cellulose from different sources are in the interval 130–198 kJ mol^{-1}, for hemicellulose in the range 95–140 kJ mol^{-1} and for lignin between 141–215 kJ mol^{-1}.

In Figs. 9a and 9d evolutions for Ea and A in cellulose–HDPE and cellulose–LDPE studied mixtures respectively are shown. Both correspond to the algebraic sum of the values of the individual components, with no synergistic effect has been observed for this component in the studied mixtures.

In the evolutions found for Ea and A in the mixtures tested with hemicellulose (Figs. 9b and 9e) a synergistic effect, with a decrease of 40 kJ mol^{-1} in the values corresponding to the 70% Hemicellulose–30% HDPE mixture and 10 kJ mol^{-1} in the values corresponding to 40% Hemicellulose–60% LDPE mixture, both with respect to 100% Hemicellulose, has been found.

Also in the evolution of Lignin–HDPE mixtures (Fig. 9c) a strong synergistic effect (a decrease of 67 kJ mol^{-1} with respect to 100% Lignin) in the values corresponding to the 70% Lignin–30% HDPE mixture has been found. Nevertheless, a lower decrease in the Lignin–LDPE has been found. In these mixtures, a decrease of 5 kJ mol^{-1} corresponding to 40% Lignin–60% LDPE), with respect to 100% Lignin, can be observed.

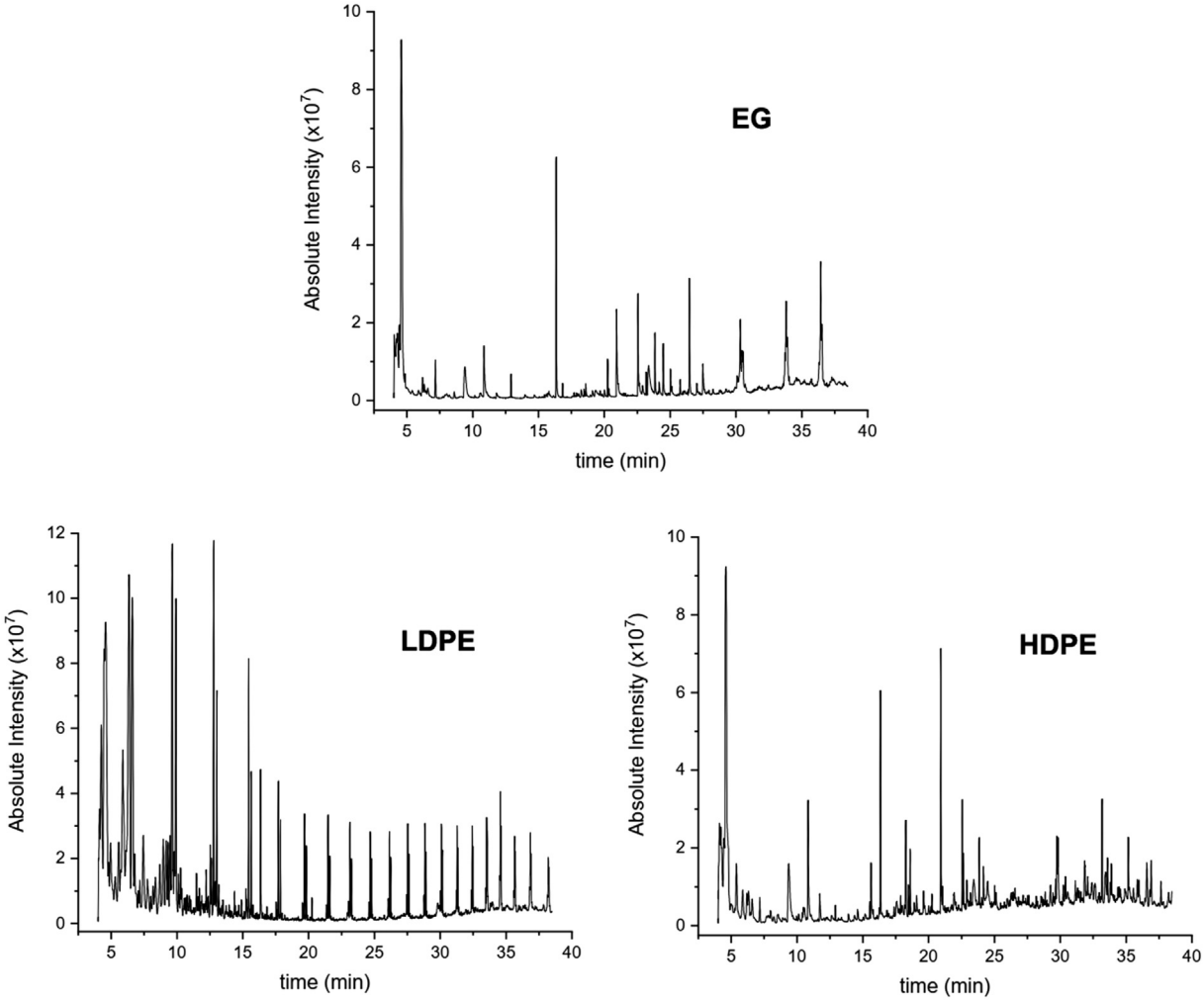

Fig. 10. Gas chromatograms at the temperature of maximum evolution during pyrolysis of EG, LDPE and HDPE.

3.7. Pyrolysis product identification by GC–MS/MS

The relative percentage of each volatile organic compound obtained at maximum evolution temperatures in the pyrolysis of EG, HDPE, LDPE and mixtures (80% EG–20% HDPE and 60% EG–40% LDPE) are shown in Table 2.

The main compounds present in the pyrolysis are n-paraffin, olefins, furans, phenols, ketones, aldehydes, esters, alcohols, and sugars. In LDPE, only n-paraffin (55%) and olefins (44%) were identified (Fig. 10). Similar results were obtained by other authors (Ballice, 2002; Ballice et al., 1998). However, n-paraffin, ketones, phenols, and sugars were the main compounds identified during the pyrolysis for both HDPE and EG (Fig. 10).

Phenols, esters, sugars, and aromatic compounds were observed when HDPE was added to the biomass. Otherwise, paraffin, olefins, ketones, furans, and alcohols were decreased in the co-pyrolysis of 80% EG–20% HDPE mixture at 316 °C. These results can indicate a synergistic effect of EG and HPDE during co-pyrolysis that favored the decomposition of hemicellulose and lignin to other compounds, such as phenols, esters and aromatic compounds. Domínguez et al. (2008) suggested that the degradation of lignin between 200–450 °C can be because lignin presents a complex structure made up of phenolic hydroxyl, carbonyl groups and benzylic hydroxyl, which are connected by straight. In addition, (Z)-Phenol, 2-methoxy-4-(1-propenyl) (Isoeugenol) and Phenol, 2,6-dimethoxy-4-(2-propenyl) are predominant phenols compounds and could be obtained from the cleavage of β-O-4 linkages in the lignin (Chen et al., 2018).

For 60% EG–40% LDPE mixture, n-paraffin, olefins, furans, phenols, ketones, esters, alcohols, sugar compounds were identified at the first degradation temperature (335 °C). However, only n-paraffin and olefins were identified using the second degradation temperature (460 °C). Adding LDPE, a synergistic effect on the formation of n-paraffin and olefins was observed at 460 °C, This can be due to the interaction between hemicellulose and lignin that usually appears below 400 °C, before the decomposition of LDPE (Yang et al., 2016).

4. Conclusions

Pyrolysis can be a technically suitable process for the valorization of *Eucalyptus globulus* mixtures with both HDPE and LDPE. Calculations ASTM-E1641 for the kinetic parameters seem to give adequate results for the tested mixtures. Minima in both the Activation Energy and in the Arrhenius Pre-exponential Factor have been found for the various mixtures under study. Thus, the EG-HDPE mixtures had a minimum for both kinetic parameters at the 80% EG–20% HDPE ratio. The minimum values for EG–LDPE mixtures in 60% EG–40% LDPE ratio have been found. In the study of mixtures of both HDPE and LDPE with the main components of Eucalyptus (cellulose, hemicellulose and lignin) no synergistic effect in the decrease of the Activation Energy for pyrolysis of cellulose has been appreciated. However, a significant

Table 2
VOCs (% area) at maximum evolution temperatures in pyrolysis of EG, HDPE, LDPE and mixtures of EG–HDPE and EG–LDPE.

	Compound name	Retention time (min)	Chemical Formula	LDPE	HDPE	EG	EG 40%–LDPE 60% (1st Peak)	EG 40%–LDPE 60% (2nd Peak)	EG 80%–HDPE 20%
1	Alkene—C7[b]	4.46	C_7H14	7.2	–	2.0	–	2.1	–
2	Alkane—C7[a]	4.53	$C_7H_{14}O$	13.9	15.8	22.4	20.3	15.5	19.2
3	2,2'-Bifuran, octahydro[c]	5.85	$C_8H_{14}O_2$	–	3.0	0.9	1.8	–	–
4	Disulfide, dimethyl[a]	5.39	$C_2H_6S_2$	–	5.5	–	–	–	0.4
5	3-Hexanone[a]	6.16	$C_6H_{12}O$	–	2.9	1.8	1.3	–	–
6	2-Hexanone[c]	6.28	$C_6H_{12}O$	–	3.1	1.5	1.6	–	–
7	Alkene—C8[a]	6.36	C_8H_{16}	8.3	–	–	–	4.0	–
8	3-Hydroperoxyhexane[c]	6.44	$C_6H_{14}O_2$	–	–	0.7	0.4	–	–
9	Alkane—C8[a]	6.57	C_8H_{18}	12.5	–	–	–	4.0	–
10	Octanal[c]	6.59	$C_8H_{16}O$	–	1.5	–	–	–	0.6
11	Furan, 2,5-dimethyl[c]	7.77	C_6H_8O	–	1.2	1.4	2.1	–	–
12	Isobutyl methyl carbonate[c]	8.62	$C_6H_{12}O_3$	–	–	0.6	–	–	16.6
13	Hexan-2,4-dione, enol[a]	9.35	$C_6H_{10}O_2$	–	15.1	10.0	6.1	–	–
14	Diene C9[a]	9.48	C_9H_{18}	4.2	–	–	–	1.1	–
15	Alkene—C9[a]	9.65	C_9H_{18}	6.0	–	–	–	0.5	–
16	Alkane—C9[a]	9.89	C_9H_{20}	8.4	–	–	–	3.4	–
17	2,5-Hexanedione[a]	10.82	$C_6H_{10}O_2$	–	14.5	15.0	11.4	–	–
18	Allyl isovalerate[c]	11.72	$C_8H_{14}O_2$	–	3.3	2.1	1.7	–	–
19	Diene C10[a]	12.53	$C_{10}H_{18}$	2.1	–	–	–	0.2	–
20	Alkene—C10[a]	12.79	$C_{10}H_{20}$	5.5	–	–	–	1.1	–
21	Alkane—C10[a]	13.03	$C_{10}H_{22}$	5.3	–	–	–	1.6	–
22	2(3H)-Furanone, 5-ethyldihydro[c]	14.60	$C_6H_{10}O_2$	–	1.0	0.6	0.7	–	–
23	Butyl isobutyl carbonate[b]	15.31	$C_9H_{18}O_3$	–	–	–	–	–	6.2
24	Diene C11[a]	15.24	$C_{11}H_{20}$	0.5	–	–	–	–	0.4
25	Alkene—C11[a]	15.44	$C_{11}H_{22}$	2.1	–	–	–	0.5	0.2
26	Phenol, 2-methoxy[a]	15.53	$C_7H_8O_2$	–	1.0	0.5	0.2	–	0.5
27	Alkane—C11[a]	15.64	$C_{11}H_{24}$	3.6	–	–	–	1.5	1.1
28	Diene C12[a]	17.53	$C_{12}H_{22}$	0.3	–	–	–	0.2	–
29	Alkene—C12[a]	17.70	$C_{12}H_{24}$	0.9	–	–	–	0.5	0.3
30	Alkane—C12[a]	17.87	$C_{12}H_{26}$	2.5	–	–	–	1.7	0.7
31	1,4:3,6-Dianhydro-alpha-d-glucopyranose[b]	18.21	$C_6H_80_4$	–	6.8	0.9	1.0	–	3.6
32	3,4-Anhydro-d-galactosan[b]	18.43	$C_6H_8O_4$	–	0.8	0.2	0.2	–	0.6
33	2,3-Anhydro-d-mannosan[b]	18.57	$C_6H_8O_4$	–	1.4	0.4	0.3	–	1.1
34	Diene C13[a]	19.54	$C_{13}H_{24}$	0.4	–	–	–	0.4	–
36	Alkene—C13[a]	19.68	$C_{13}H_{26}$	0.8	–	–	–	0.9	–
37	Alkane—C13[a]	19.83	$C_{13}H_{28}$	1.7	–	–	–	2.3	0.4
38	2-Methoxy-4-vinylphenol[c]	20.30	$C_9H_{10}O_2$	–	0.1	0.8	0.5	–	1.4
39	Phenol, 2,6-dimethoxy[a]	20.91	$C_7H_8O_2$	–	7.5	7.3	7.3	–	8.3
40	Diene C14[a]	21.35	$C_{14}H_{26}$	0.3	–	–	–	0.6	–
41	Alkene—C14[c]	21.48	$C_{14}H_{28}$	0.8	–	–	–	1.9	0.1
42	Alkane—C14[a]	21.61	$C_{14}H_{30}$	1.4	–	–	–	3.1	0.2
43	2,5-Dimethoxybenzyl alcohol[c]	22.54	$C_8H_{10}O_3$	–	3.8	5.9	4.4	–	4.0
44	(Z)-Phenol, 2-methoxy-4-(1-propenyl)[c]	22.63	$C_{10}H_{12}O_2$	–	1.6	0.7	1.0	–	1.8
45	Diene C15[a]	23.02	$C_{15}H_{28}$	0.3	–	0.5	–	1.1	0.1
46	Alkene—C15[a]	23.14	$C_{15}H_{30}$	0.8	–	–	–	3.1	0.1
47	Alkane—C15[a]	23.25	$C_{15}H_{32}$	1.3	–	3.7	–	4.2	–
48	5-tert-Butylpyrogallol c	23.82	$C_{10}H_{14}O_3$	–	2.8	4.1	4.7	–	4.7
49	2-Propanone, 1-(4-hydroxy-3-methoxyphenyl)[c]	24.00	$C_{10}H_{12}O_3$	–	0.6	0.6	1.5	–	1.6
50	3,5-Dimethoxyacetophenone[c]	24.45	$C_{10}H_{12}O_3$	–	–	3.0	2.9	–	7.4
51	Diene C16[a]	24.58	$C_{16}H_{30}$	0.3	–	–	–	1.7	–
52	Alkene—C16[a]	24.69	$C_{16}H_{32}$	0.7	–	–	–	3.6	–
53	Alkane—C16[a]	24.79	$C_{16}H_{34}$	1.3	–	–	–	4.5	0.1
54	Phenol, 2,6-dimethoxy-4-(2-propenyl)[c]	25.00	$C_{11}H_{14}O_3$	–	0.3	0.8	1.3	–	1.7
55	Phenol, 2,6-dimethoxy-4-(2-propenyl)[c]	26.45	$C_{11}H_{14}O_3$	–	0.1	4.3	5.3	–	6.8
56	Ethanone, 1-(4-hydroxy-3,5-dimethoxyphenyl)[b]	26.97	$C_{10}H_{12}O_4$	–	–	1.2	2.6	–	1.6
57	Diene C17[a]	26.05	$C_{17}H_{32}$	0.3	–	–	–	2.2	–
58	Alkene—C17[a]	26.15	$C_{17}H_{34}$	0.7	–	–	–	4.0	–
59	Alkane—C17[a]	26.24	$C_{17}H_{36}$	1.3	–	–	–	4.7	0.1
60	2-Propenal, 3-(4-hydroxy-3-methoxyphenyl)[c]	27.14	$C_{10}H_{10}O_3$	–	–	–	0.5	–	–
61	Diene C18[a]	27.44	$C_{18}H_{34}$	0.3	–	–	–	2.5	–
62	Desaspidino[c]	27.45	$C_{11}H_{14}O_4$	–	0.1	4.4	7.2	–	6.7
63	Alkene—C18[a]	27.53	$C_{18}H_{36}$	0.8	–	–	–	4.5	–
64	Alkane—C18[a]	27.61	$C_{18}H_{38}$	1.2	–	–	–	4.6	–
65	Diene C19[a]	28.76	$C_{19}H_{36}$	0.2	–	–	–	2.9	–
66	Alkene—C19[a]	28.84	$C_{19}H_{38}$	0.8	–	–	–	4.5	–
67	Alkane—C19[a]	28.92	$C_{19}H_{40}$	1.2	–	–	–	4.9	–
68	Hexanamide, N-tetrahydrofurfuryl[c]	36.56	$C_{10}H_{19}NO_2$	–	4.7	–	6.3	–	–
69	Squalene[a]	37.63	$C_{30}H_{50}$	–	1.5	–	4.1	–	–
70	1-bromo-3-chlorobenzene (internal standard)[a]	16.34	C_6H_4BrCl						

[a]Compounds identified with more than 95% similarity to the NIST11 library spectra.
[b]Compounds identified with more than 90% similarity to the NIST11 library spectra.
[c]Compounds identified with more than 85% similarity to the NIST11 library spectra.

decrease in the Activation Energy is observed for mixtures of both hemicellulose and lignin with both types of polyethylene. Therefore, the lowest activation energies with both hemicellulose and lignin for 60% EG–40% HDPE and 40% EG–60% LDPE have been found. Thus, the lowering of both the Activation Energy and the Arrhenius pre-exponential factor in eucalyptus with polyethylene mixtures to the presence of hemicellulose and lignin could be attributed.

The main VOCs identified in the pyrolysis of HDPE and EG samples were n-paraffins, ketones, phenols and sugars. In contrast, in LDPE, only n-paraffins (55%) and olefins (44%) were identified. Characterizations of the material, including FTIR, could help to identify the functional groups involved in the synergistic effects found.

The optimum mixture for co-pyrolysis of EG–HDPE corresponds to 60% EG and 40% HDPE and for co-pyrolysis of EG–LDPE mixtures is 40% EG and 60% LDPE.

CRediT authorship contribution statement

M. Ruiz-Montoya: Conceptualization, Methodology, Investigation, Formal analysis, Supervision, Writing - review & editing. **A. Palma:** Conceptualization, Methodology, Investigation, Formal analysis, Data curation, Writing – original draft, Supervision, Visualization. **S. Lozano-Calvo:** Investigation, Formal analysis, Data curation, Visualization. **E. Morales:** Methodology, Investigation, Data curation, Supervision. **M.J. Díaz:** Conceptualization, Methodology, Investigation, Funding acquisition, Supervision, Writing – review & editing, Project administration.

Declaration of competing interest

The authors declare that they have no known competing financial interests or personal relationships that could have appeared to influence the work reported in this paper.

Data availability

No data was used for the research described in the article.

Acknowledgments

This study received financial support from Green Asphalt project (ref. 802C1800001) co-funded 80% by FEDER European Programme and 20% by the Regional Government of Andalusia (Agency for Innovation and Development of Andalusia (IDEA) and (Operational Programme FEDER Andalusia 2014–2020, Project UHU–1255540), Spain.

References

Aboulkas, A., El harfi, K., El Bouadili, A., 2010. Thermal degradation behaviors of polyethylene and polypropylene. Part I: Pyrolysis kinetics and mechanisms. Energy Convers. Manag. 51, 1363–1369. http://dx.doi.org/10.1016/J.ENCONMAN.2009.12.017.

Al-Yaari, M., Dubdub, I., 2020. Application of artificial neural networks to predict the catalytic pyrolysis of HDPE using non-isothermal TGA data. Polym 12 (1813), http://dx.doi.org/10.3390/POLYM12081813, 2020, 12, 1813.

Alam, M., Bhavanam, A., Jana, A., Viroja, S., Peela, N.R., 2020. Co-pyrolysis of bamboo sawdust and plastic: Synergistic effects and kinetics. Renew. Energy 149, 1133–1145. http://dx.doi.org/10.1016/J.RENENE.2019.10.103.

Antelava, A., Jablonska, N., Constantinou, A., Manos, G., Salaudeen, S.A., Dutta, A., Al-Salem, S.M., 2021. Energy potential of plastic waste valorization: A short comparative assessment of pyrolysis versus gasification. Energy Fuels 35, 3558–3571. http://dx.doi.org/10.1021/ACS.ENERGYFUELS.0C04017.

Balaji, A.B., Liu, X., 2021. Plastics in circular economy: A sustainable progression. Introd. Circ. Econ. 15, 9–178. http://dx.doi.org/10.1007/978-981-15-8510-4_9.

Ballice, L., 2002. Classification of volatile products evolved during temperature-programmed co-pyrolysis of low-density polyethylene (LDPE) with polypropylene (PP). Fuel 81, 1233–1240. http://dx.doi.org/10.1016/S0016-2361(01)00130-2.

Ballice, L., Yüksel, M., Sağlam, M., Reimert, R., Schulz, H., 1998. Classification of volatile products evolved during temperature-programmed co-pyrolysis of Turkish oil shales with low density polyethylene. Fuel 77, 1431–1441. http://dx.doi.org/10.1016/S0016-2361(98)00066-0.

Barneto, A.G., Vila, C., Ariza, J., 2011. Eucalyptus kraft pulp production: Thermogravimetry monitoring. Thermochim. Acta 520, 110–120. http://dx.doi.org/10.1016/J.TCA.2011.03.027.

Barrio-Anta, M., Castedo-Dorado, F., Cámara-Obregón, A., López-Sánchez, C.A., 2021. Integrating species distribution models at forest planning level to develop indicators for fast-growing plantations. a case study of Eucalyptus globulus Labill. in Galicia (NW Spain). Forest Ecol. Manag. 491, 119200. http://dx.doi.org/10.1016/J.FORECO.2021.119200.

Bishop, G., Styles, D., Lens, P.N., 2020. Recycling of European plastic is a pathway for plastic debris in the ocean. Environ. Int 142, 105893. http://dx.doi.org/10.1016/J.ENVINT.2020.105893.

Bueno, P., Tapias, R., López, F., Díaz, M., 2008. Optimizing composting parameters for nitrogen conservation in composting. Bioresour. Technol. 99, 5069–5077. http://dx.doi.org/10.1016/J.BIORTECH.2007.08.087.

Burra, K.G., Gupta, A.K., 2018. Kinetics of synergistic effects in co-pyrolysis of biomass with plastic wastes. Appl. Energy 220, 408–418. http://dx.doi.org/10.1016/J.APENERGY.2018.03.117.

Chattopadhyay, J., Pathak, T.S., Srivastava, R., Singh, A.C., 2016. Catalytic co-pyrolysis of paper biomass and plastic mixtures (HDPE (high density polyethylene), PP (polypropylene) and PET (polyethylene terephthalate)) and product analysis. Energy 103, 513–521. http://dx.doi.org/10.1016/J.ENERGY.2016.03.015.

Chen, D., Gao, A., Cen, K., Zhang, J., Cao, X., Ma, Z., 2018. Investigation of biomass torrefaction based on three major components: Hemicellulose, cellulose, and lignin. Energy Convers. Manag. 169, 228–237. http://dx.doi.org/10.1016/j.enconman.2018.05.063.

Chen, R., Zhang, S., Cong, K., Li, Q., Zhang, Y., 2020. Insight into synergistic effects of biomass-polypropylene co-pyrolysis using representative biomass constituents. Bioresour. Technol. 307, 123243. http://dx.doi.org/10.1016/J.BIORTECH.2020.123243.

Cheng, Q., Jiang, M., Qin, Z., Zhang, S., Wang, M., Li, J., 2017. Thermogravimetry study of the pyrolytic characteristics and kinetics of fast-growing Eucalyptus residue. Energy Fuels 31, 13675–13681. http://dx.doi.org/10.1021/ACS.ENERGYFUELS.7B02363.

Cheng, K., Winter, W.T., Stipanovic, A.J., 2012. A modulated-TGA approach to the kinetics of lignocellulosic biomass pyrolysis/combustion. Polym. Degrad. Stab. 97, 1606–1615. http://dx.doi.org/10.1016/J.POLYMDEGRADSTAB.2012.06.027.

Chow, C., Wong, W., Chan, CW, Chan, CS, 2018. Converting inert plastic waste into energetic materials: A study on the light-accelerated decomposition of plastic waste with the fenton reaction. Waste Manage. 75, 174–180. http://dx.doi.org/10.1016/J.WASMAN.2018.01.034.

Clauser, N.M., González, G., Mendieta, C.M., Kruyeniski, J., Area, M.C., Vallejos, M.E., 2021. Biomass waste as sustainable raw material for energy and fuels. Sustain 13, 794. http://dx.doi.org/10.3390/SU13020794, 2021, 13, 794.

Conesa, J.A., Font, R., Marcilla, A., Caballero, J.A., 1997. Kinetic model for the continuous pyrolysis of two types of polyethylene in a fluidized bed reactor. J. Anal. Appl. Pyrolysis 40–41, 419–431. http://dx.doi.org/10.1016/S0165-2370(97)00033-8.

da Silva, J., Alves, J., Galdino, W., Andersen, S., de Sena, R., 2017. Pyrolysis kinetic evaluation by single-step for waste wood from reforestation. Waste Manage. 72, 265–273. http://dx.doi.org/10.1016/J.WASMAN.2017.11.034.

Dantas, G.A., Legey, L.F.L., Mazzone, A., 2013. Energy from sugarcane bagasse in Brazil: An assessment of the productivity and cost of different technological routes. Renew. Sustain. Energy Rev 21, 356–364. http://dx.doi.org/10.1016/J.RSER.2012.11.080.

Dar, R.A., Parmar, M., Dar, E.A., Sani, R.K., Phutela, U.G., 2021. Biomethanation of agricultural residues: Potential, limitations and possible solutions. Renew. Sustain. Energy Rev. 135, 110217. http://dx.doi.org/10.1016/J.RSER.2020.110217.

Delgado-Rodríguez, M., Ruiz-Montoya, M., Giraldez, I., Cabeza, I., López, R., Díaz, M., 2010. Effect of control parameters on emitted volatile compounds in municipal solid waste and pine trimmings composting. J. Environ. Sci. Health. A. Tox. Hazard. Subst. Environ. Eng. 45, 855–862. http://dx.doi.org/10.1080/10934521003709057.

Díaz, M.J., Ruiz-Montoya, M., Palma, A., de Paz, M.-V., 2021. Thermogravimetry applicability in compost and composting research: A review. Appl. Sci. 11 (1692), http://dx.doi.org/10.3390/APP11041692, 2021, 11, 1692.

Domínguez, M., Madejón, P., Madejón, E., Diaz, M., 2017. Novel energy crops for mediterranean contaminated lands: Valorization of Dittrichia viscosa and Silybum marianum biomass by pyrolysis. Chemosphere 186, 968–976. http://dx.doi.org/10.1016/J.CHEMOSPHERE.2017.08.063.

Domínguez, J.C., Oliet, M., Alonso, M.V., Gilarranz, M.A., Rodríguez, F., 2008. Thermal stability and pyrolysis kinetics of organosolv lignins obtained from eucalyptus globulus. Ind. Crops Prod. 27, 150–156. http://dx.doi.org/10.1016/J.INDCROP.2007.07.006.

Dou, B., Lim, S., Kang, P., Hwang, J., Song, S., Yu, T., Kyoon-Duk, Y., 2007. Kinetic study in modeling pyrolysis of refuse plastic fuel. Energy Fuels 21, 1442–1447. http://dx.doi.org/10.1021/EF060594C.

Duque, J.V., Martins, M.F., Debenest, G., Orlando, M.T., 2020. The influence of the recycling stress history on LDPE waste pyrolysis. Polym. Test 86, 106460. http://dx.doi.org/10.1016/J.POLYMERTESTING.2020.106460.

Dussan, K., Dooley, S., Monaghan, R., 2017. Integrating compositional features in model compounds for a kinetic mechanism of hemicellulose pyrolysis. Chem. Eng. J. 328, 943–961. http://dx.doi.org/10.1016/J.CEJ.2017.07.089.

Fa, W., Wang, J., Ge, S., Chao, C., 2019. Performance of photo-degradation and thermo-degradation of polyethylene with photo-catalysts and thermo-oxidant additives. Polym. Bull. 773 (77), 1417–1432. http://dx.doi.org/10.1007/S00289-019-02813-Z, 2019.

FAO, 2022. Food and agriculture organization of the united nations. In: The State of the World's Forests 2022. Working paper of Electronic Publishing Policy and Support Branch, https://www.fao.org/publications/sofo/2022/en/.

Ferreira, A.F., 2017. Biorefinery concept. Lect. Notes Energy 57, 1–20. http://dx.doi.org/10.1007/978-3-319-48288-0_1.

Galano, A., Aburto, J., Sadhukhan, J., Torres-García, E., 2017. A combined theoretical-experimental investigation on the mechanism of lignin pyrolysis: Role of heating rates and residence times. J. Anal. Appl. Pyrolysis 128, 208–216. http://dx.doi.org/10.1016/J.JAAP.2017.10.009.

Garrote, G., Parajó, J.C., 2002. Non-isothermal autohydrolysis of Eucalyptus wood. Wood Sci. Technol. 36, 111–123. http://dx.doi.org/10.1007/s00226-001-0132-2.

Ge, S., Yek, P.N., Cheng, Y.W., Xia, C., Wan Mahari, W.A., Liew, R.K., Peng, W., Yuan, T.Q., Tabatabaei, M., Aghbashlo, M., Sonne, C., Lam, S.S., 2021. Progress in microwave pyrolysis conversion of agricultural waste to value-added biofuels: A batch to continuous approach. Renew. Sustain. Energy Rev. 135, 110148. http://dx.doi.org/10.1016/J.RSER.2020.110148.

Hassan, H., Hameed, B.H., Lim, J.K., 2020. Co-pyrolysis of sugarcane bagasse and waste high-density polyethylene: Synergistic effect and product distributions. Energy 191, 116545. http://dx.doi.org/10.1016/J.ENERGY.2019.116545.

Junmeng, C., Siyu, C., 2009. A new iterative linear integral isoconversional method for the determination of the activation energy varying with the conversion degree. J. Comput. Chem. 30, 1986–1991. http://dx.doi.org/10.1002/JCC.21195.

Kai, X., Yang, T., Shen, S., Li, R., 2019. TG-FTIR-MS study of synergistic effects during co-pyrolysis of corn stalk and high-density polyethylene (HDPE). Energy Convers. Manag. 181, 202–213. http://dx.doi.org/10.1016/J.ENCONMAN.2018.11.065.

Khalturinskii, N.A., 1987. High-temperature pyrolysis of polymers. J. Therm. Anal. 326 (32), 1675–1682. http://dx.doi.org/10.1007/BF01913945, 1987.

Lei, Z., Wang, S., Fu, H., Gao, W., Wang, B., Zeng, J., Xu, J., 2019. Thermal pyrolysis characteristics and kinetics of hemicellulose isolated from Camellia Oleifera shell. Bioresour. Technol. 282, 228–235. http://dx.doi.org/10.1016/J.BIORTECH.2019.02.131.

Leng, L., Huang, H., 2018. An overview of the effect of pyrolysis process parameters on biochar stability. Bioresour. Technol. 270, 627–642. http://dx.doi.org/10.1016/J.BIORTECH.2018.09.030.

Leschinsky, M., Sixta, H., Patt, R., 2009. Detailed mass balances of the autohydrolysis of eucalyptus globulus at 170 °c. BioResources 4, 687–703. http://dx.doi.org/10.15376/biores.4.2.687-703.

Lin, Y.-C., Cho, J., Tompsett, G.A., Westmoreland, P.R., Huber, G.W., 2009. Kinetics and mechanism of cellulose Pyrolysis. J. Phys. Chem. C 113, 20097–20107. http://dx.doi.org/10.1021/JP906702P.

Lu, Q., Xie, W., luan, Hu, B., Liu, J., Zhao, W., Zhang, B., Wang, T., peng, 2021. A novel interaction mechanism in lignin pyrolysis: Phenolics-assisted hydrogen transfer for the decomposition of the β-O-4 linkage. Combust. Flame 225, 395–405. http://dx.doi.org/10.1016/J.COMBUSTFLAME.2020.11.011.

Miranda, I., Gominho, J., Mirra, I., Pereira, H., 2013. Fractioning and chemical characterization of barks of Betula pendula and Eucalyptus globulus. Ind. Crops Prod. 41, 299–305. http://dx.doi.org/10.1016/j.indcrop.2012.04.024.

Mishra, R., Mohanty, K., 2018. Pyrolysis kinetics and thermal behavior of waste sawdust biomass using thermogravimetric analysis. Bioresour. Technol. 251, 63–74. http://dx.doi.org/10.1016/J.BIORTECH.2017.12.029.

Mishra, R.K., Sahoo, A., Mohanty, K., 2019. Pyrolysis kinetics and synergistic effect in co-pyrolysis of Samanea saman seeds and polyethylene terephthalate using thermogravimetric analyser. Bioresour. Technol. 289, 121608. http://dx.doi.org/10.1016/J.BIORTECH.2019.121608.

Mumbach, G.D., Alves, J.L., Da Silva, J.C., De Sena, R.F., Marangoni, C., Machado, R.A., Bolzan, A., 2019. Thermal investigation of plastic solid waste pyrolysis via the deconvolution technique using the asymmetric double sigmoidal function: Determination of the kinetic triplet, thermodynamic parameters, thermal lifetime and pyrolytic oil composition for clean. Energy Convers. Manag. 200, 112031. http://dx.doi.org/10.1016/J.ENCONMAN.2019.112031.

Navarro, M.V., López, J.M., Veses, A., Callén, M.S., García, T., 2018. Kinetic study for the co-pyrolysis of lignocellulosic biomass and plastics using the distributed activation energy model. Energy 165, 731–742. http://dx.doi.org/10.1016/J.ENERGY.2018.09.133.

Oyedun, A.O., Tee, C.Z., Hanson, S., Hui, C.W., 2014. Thermogravimetric analysis of the pyrolysis characteristics and kinetics of plastics and biomass blends. Fuel Process. Technol. 128, 471–481. http://dx.doi.org/10.1016/J.FUPROC.2014.08.010.

Ozawa, T., 1965. A new method of analyzing thermogravimetric data. Bull. Chem. Soc. Jpn. 38, 1881–1886. http://dx.doi.org/10.1246/bcsj.38.1881.

Patil, V., Adhikari, S., Cross, P., 2018. Co-pyrolysis of lignin and plastics using red clay as catalyst in a micro-pyrolyzer. Bioresour. Technol. 270, 311–319. http://dx.doi.org/10.1016/J.BIORTECH.2018.09.034.

Pazienza, P., De Lucia, C., 2020. For a new plastics economy in agriculture: Policy reflections on the EU strategy from a local perspective. J. Clean. Prod. 253, 119844. http://dx.doi.org/10.1016/J.JCLEPRO.2019.119844.

Pérez-Cruzado, C., Merino, A., Rodríguez-Soalleiro, R., 2011. A management tool for estimating bioenergy production and carbon sequestration in Eucalyptus globulus and Eucalyptus nitens grown as short rotation woody crops in north-west Spain. Biomass Bioenergy 35, 2839–2851. http://dx.doi.org/10.1016/J.BIOMBIOE.2011.03.020.

Poletto, M., Zattera, A.J., Forte, M.M., Santana, R.M., 2012. Thermal decomposition of wood: Influence of wood components and cellulose crystallite size. Bioresour. Technol. 109, 148–153. http://dx.doi.org/10.1016/J.BIORTECH.2011.11.122.

Popp, J., Kovács, S., Oláh, J., Divéki, Z., Balázs, E., 2021. Bioeconomy: Biomass and biomass-based energy supply and demand. N. Biotechnol. 60, 76–84. http://dx.doi.org/10.1016/J.NBT.2020.10.004.

Pradhan, D., Volli, V., Singh, R.K., Murgun, S., 2020. Co-pyrolysis behavior, engine performance characteristics, and thermodynamics of liquid fuels from mahua seeds and waste thermocol: A comprehensive study. Chem. Eng. J. 393, 124749. http://dx.doi.org/10.1016/J.CEJ.2020.124749.

Quan, C., Gao, N., Song, Q., 2016. Pyrolysis of biomass components in a TGA and a fixed-bed reactor: Thermochemical behaviors, kinetics, and product characterization. J. Anal. Appl. Pyrolysis 121, 84–92. http://dx.doi.org/10.1016/J.JAAP.2016.07.005.

Rencoret, J., Gutiérrez, A., Nieto, L., Jiménez-Barbero, J., Faulds, C.B., Kim, H., Ralph, J., Martínez, Á.T., del Río, J.C., 2011. Lignin composition and structure in young versus adult eucalyptus globulus plants. Plant Physiol. 155, 667–682. http://dx.doi.org/10.1104/pp.110.167254.

Rodríguez-Luna, L., Bustos-Martínez, D., Valenzuela, E., 2021. Two-step pyrolysis for waste HDPE valorization. Process Saf. Environ. Prot. 149, 526–536. http://dx.doi.org/10.1016/J.PSEP.2020.11.038.

Ruvolo-Filho, A., Curti, P.S., 2006. Chemical kinetic model and thermodynamic compensation effect of Alkaline hydrolysis of waste poly(ethylene terephthalate) in nonaqueous Ethylene Glycol solution. Ind. Eng. Chem. Res. 45, 7985–7996. http://dx.doi.org/10.1021/IE060528Y.

Saha, B., Ghoshal, A.K., 2007. Model-free kinetics analysis of ZSM-5 catalyzed pyrolysis of waste LDPE. Thermochim. Acta 453, 120–127. http://dx.doi.org/10.1016/J.TCA.2006.11.012.

Shakoor, A., Shahzad, S., Chatterjee, N., Arif, M., Farooq, T., Altaf, M., Tufail, M., Dar, A., Mehmood, T., 2021. Nitrous oxide emission from agricultural soils: Application of animal manure or biochar? A global meta-analysis. J. Environ. Manag. 285, http://dx.doi.org/10.1016/J.JENVMAN.2021.112170.

Shen, D.K., Gu, S., Bridgwater, A.V., 2010. Study on the pyrolytic behaviour of xylan-based hemicellulose using TG–FTIR and Py–GC–FTIR. J. Anal. Appl. Pyrolysis 87, 199–206. http://dx.doi.org/10.1016/J.JAAP.2009.12.001.

Shukry, N., Ishak, F., Sefain, Z., 1991. DTA study of thermal degradation of bagasse and rice straw hemicelluloses. J. Therm. Anal. 375 (37), 915–926. http://dx.doi.org/10.1007/BF01932789, 1991.

Simmons, A.T., Cowie, A.L., Waters, C.M., 2021. Pyrolysis of invasive woody vegetation for energy and biochar has climate change mitigation potential. Sci. Total Environ. 770, 145278. http://dx.doi.org/10.1016/J.SCITOTENV.2021.145278.

Sinfrônio, F.S., Santos, J.C., Pereira, L.G., Souza, A.G., Conceição, M.M., Fernandes, Jr., V.J., Fonseca, V.M., 2005. Kinetic of thermal degradation of low-density and high-density polyethylene by non-isothermal thermogravimetry. J. Therm. Anal. Calorim. 792 (79), 393–399. http://dx.doi.org/10.1007/S10973-005-0072-4, 2005.

Singh, S., Patil, T., Tekade, S.P., Gawande, M.B., Sawarkar, A.N., 2021. Studies on individual pyrolysis and co-pyrolysis of corn cob and polyethylene: Thermal degradation behavior, possible synergism, kinetics, and thermodynamic analysis. Sci. Total Environ. 783, 147004. http://dx.doi.org/10.1016/J.SCITOTENV.2021.147004.

TAPPI Test Method T 249 cm-85, 1985. Carbohydrate composition of extractive-free wood and wood pulp by Gas-Liquid Chromatography. In: TAPPI Test Methods, Atlanta, G.A: Technical Association of the Pulp and Paper Industry.

TAPPI Test Method T 257 cm-02, 2012. Sampling and Preparing Wood for Analysis. In: TAPPI Test Methods, Atlanta, G.A: Technical Association of the Pulp and Paper Industry.

Van de Velden, M., Baeyens, J., Brems, A., Janssens, B., Dewil, R., 2010. Fundamentals, kinetics and endothermicity of the biomass pyrolysis reaction. Renew. Energy 35, 232–242. http://dx.doi.org/10.1016/J.RENENE.2009.04.019.

Vimalathithan, P.K., Barile, C., Casavola, C., Arunachalam, S., Battisti, M.G., Friesenbichler, W., Vijayakumar, C.T., 2019. Thermal degradation kinetics of polypropylene/clay nanocomposites prepared by injection molding compounder. Polym. Compos 40, 3634–3643. http://dx.doi.org/10.1002/PC.25226.

Vuthaluru, H.B., 2004. Thermal behaviour of coal/biomass blends during co-pyrolysis. Fuel Process. Technol. 85, 141–155. http://dx.doi.org/10.1016/S0378-3820(03)00112-7.

Wang, Z., Burra, K.G., Lei, T., Gupta, A.K., 2021. Co-pyrolysis of waste plastic and solid biomass for synergistic production of biofuels and chemicals-a review. Prog. Energy Combust. Sci. 84, 100899. http://dx.doi.org/10.1016/J.PECS.2020.100899.

Willems, P.A., Froment, G.F., 2002. Kinetic modeling of the thermal cracking of hydrocarbons. 2. Calculation of activation energies. Ind. Eng. Chem. Res. 27, 1966–1971. http://dx.doi.org/10.1021/IE00083A002.

Xiao, R., Yang, W., Cong, X., Dong, K., Xu, J., Wang, D., Yang, X., 2020. Thermogravimetric analysis and reaction kinetics of lignocellulosic biomass pyrolysis. Energy 201, 117537. http://dx.doi.org/10.1016/J.ENERGY.2020.117537.

Xu, Y., Chen, B., 2013. Investigation of thermodynamic parameters in the pyrolysis conversion of biomass and manure to biochars using thermogravimetric analysis. Bioresour. Technol. 146, 485–493. http://dx.doi.org/10.1016/J.BIORTECH.2013.07.086.

Xue, J., Ceylan, S., Goldfarb, J.L., 2015. Synergism among biomass building blocks? Evolved gas and kinetics analysis of starch and cellulose co-pyrolysis. Thermochim. Acta 618, 36–47. http://dx.doi.org/10.1016/J.TCA.2015.09.002.

Yang, J., Rizkiana, J., Widayatno, W.B., Karnjanakom, S., Kaewpanha, M., Hao, X., Abudula, A., Guan, G., 2016. Fast co-pyrolysis of low density polyethylene and biomass residue for oil production. Energy Convers. Manag. 120, 422–429. http://dx.doi.org/10.1016/j.enconman.2016.05.008.

Yang, H., Yan, R., Chen, H., Lee, D.H., Zheng, C., 2007. Characteristics of hemicellulose, cellulose and lignin pyrolysis. Fuel 86, 1781–1788. http://dx.doi.org/10.1016/J.FUEL.2006.12.013.

Yeo, J.Y., Chin, B.L., Tan, J.K., Loh, Y.S., 2019. Comparative studies on the pyrolysis of cellulose, hemicellulose, and lignin based on combined kinetics. J. Energy Inst. 92, 27–37. http://dx.doi.org/10.1016/J.JOEI.2017.12.003.

Yuan, H., Fan, H., Shan, R., He, M., Gu, J., Chen, Y., 2018. Study of synergistic effects during co-pyrolysis of cellulose and high-density polyethylene at various ratios. Energy Convers. Manag. 157, 517–526. http://dx.doi.org/10.1016/J.ENCONMAN.2017.12.038.

Zhang, X.M., Elkoun, S., Ajji, A., Huneault, M.A., 2004. Oriented structure and anisotropy properties of polymer blown films: HDPE, LLDPE and LDPE. Polymer (Guildf). 45, 217–229. http://dx.doi.org/10.1016/J.POLYMER.2003.10.057.

Zhang, Y., Ji, G., Ma, D., Chen, C., Wang, Y., Wang, W., Li, A., 2020. Exergy and energy analysis of pyrolysis of plastic wastes in rotary kiln with heat carrier. Process Saf. Environ. Prot. 142, 203–211. http://dx.doi.org/10.1016/J.PSEP.2020.06.021.

Zhang, X., Lei, H., Zhu, L., Zhu, X., Qian, M., Yadavalli Wu, J., Chen, S., 2016. Thermal behavior and kinetic study for catalytic co-pyrolysis of biomass with plastics. Bioresour. Technol. 220, 233–238. http://dx.doi.org/10.1016/J.BIORTECH.2016.08.068.

Zhou, L., Wang, Y., Huang, Q., Cai, J., 2006. Thermogravimetric characteristics and kinetic of plastic and biomass blends co-pyrolysis. Fuel Process. Technol. 87, 963–969. http://dx.doi.org/10.1016/J.FUPROC.2006.07.002.